Flexural Behavior of Preflex SFRC-Encased Steel Joist Composite Beams

Presented To the Faculty of the Graduate School of

The University of Texas at Arlington in Partial Fulfillment

of the Requirements for the Degree of

Master of Science in Civil Engineering

THE UNIVERSITY OF TEXAS AT ARLINGTON

May 2019

Acknowledgements

I would like to express my thanks to Dr. Azzawi for his invaluable support and counsel throughout this research. Dr. Azzawi's mentorship has guided my educational and professional growth. I appreciate the time and effort he has instilled in my progression through the program and the completion of my thesis. I am grateful to Dr. Kermanshachi and Dr. Sabatino for their cooperation and guidance on the defense committee.

I would also like to thank my parents for their love and support and my two sisters who have always encouraged and uplifted me.

May 2, 2019

Abstract

Surpervising Professor: Dr. Raad K. Azzawi

This research investigates the behavior of encased steel composite beams within steel fiber reinforced concrete (SFRC) in straight and preflex beams, using nonlinear analysis. ABAQUS FEA software has been adopted. Composite steel beams encased in fiber reinforced concrete are analyzed and a comparison is made with available experimental results. Good agreement with the experimental results is observed. Upwards camber of the steel section is introduced on the steel joist. It's found that the preflex section can increase the ultimate load capacity by 10% and decrease midspan displacement by 13% of the same beams without the preflex steel section. Steel fiber dosages, compressive strength, modulus of rupture are examined. The effect of cambering and mesh refinement are also investigated. The physical properties of SFRC are calculated through testing at the UTA Civil Engineering Laboratory Building. In total, nine (4" x 8") cylindrical specimens, nine (6" x 8") cylindrical specimens, and nine (6" x 6" x 20") beam specimens were produced and tested for their compressive strength, tensile strength, and modulus of rupture after 28 days of curing. The addition of steel fiber will lead to a significant increase in tensile strength and modulus of rupture of concrete. Adding 1% steel fibers by volume can increase the load capacity by 33% and decrease the midspan displacement by 70% in comparison to the same beam using plain concrete. The increase in steel fibers and cambering show an improvement to the flexural capacity and cracking point of the beam, which can provide more strength to structures such as long span bridges.

Table of Contents

List of Illustrations

List of Tables

Chapter 1

Introduction

Preflex beams can improve the design of many structures in Civil Engineering. Bridge structures such as highways and railways require long span girders of high strength. High-rise structures such as the Tour du Midi (1967) in Belgium use preflex beams because of its compressive and tensile benefits. These beams have large load bearing capacities and perform well in flexural behavior. Therefore, the expansion of research on preflex beams with the incorporation of SFRC can improve its flexural strength.

Preflex girders are an innovative composite member that can support bridges and buildings that experience large service loads. There is a limited amount of research in this field, especially as it pertains to Preflex SFRC encased steel beams. SFRC improves the material properties of the encasement so that the beam has a higher compression strength and modulus of rupture. Upward cambering increases the flexural behavior by introducing preflexion loads to the steel portion of the beam before construction. Encasing the beam with the SFRC while under this tension creates the composite beam. This preflex hybrid structure contains all the properties that are beneficial from concrete and steel.

Research is progressively expanding on the benefits of preflex beams and SFRC. The exploration of the two innovations in one composite structure provides better performance in flexural strength and less construction efforts and cost.

1.1 Objectives

The objective of this research is composed of two primary goals. The first is to analyze a SFRC encased steel joist straight beam under flexural load. Then compare the load-displacement results from FEA to Khuntia and Goel's experiment on a SFRC encased steel joist composite beam [14]. The first objective is to confirm using FEA that the results are close to the experimental study. This confirmation allows for FEA to be utilized for the second objective of this research. The second objective consists of a parametric study completed in two parts. The first part is to analyze a straight beam under flexural load for three cases; 0%, 0.5%, and 1% SFRC. The second part is to preflex the beam and analyze it for the same parameters of steel fiber as done for the straight beam. Targets for each parametric study are to collect the load-displacement values from FEA to see how steel fibers and cambering contribute to a change in load

capacity and to the midspan displacement. In order to accomplish these objectives, a laboratory testing of the SFRC material is done to find the compression, modulus of rupture, and tensile strength. The compressive strength and modulus of rupture are the main parameters in FEA that defines each case.

1.2 Research Contribution

Bridge design industries will benefit from the research development of this field in order to save cost and design efforts for structures such as long spanning bridge girders. Various design codes such as ACI (American Concrete Institute), ASCE (American Society of Civil Engineers), and AASHTO (American Association of State Highway and Transportation) have limited research on Preflex SFRC Encased Steel Composite Beams. Available experiments of this type of beam are beneficial especially for long span bridges girders. Camber in a beam can increase its flexural capacity and improve bridges that require high load bearing capacity girders. Preflex beam girders are lighter than commonly used prestressed concrete beams and experience less deflection. Bridge-design industries will also find a decrease in construction costs and labor with the use of Preflex SFRC Encased Steel Composite Beams. Operation is made simpler because preflex technology can be applied during fabrication. More research on the benefits of preflex composite beams can improve on the results found and discussed in this study.

1.3 Outline for Thesis

This thesis is organized into the following chapters:

Chapter 1- Introduction: Defines the two major studies that this research focuses on, and the approaches that will be taken to achieve each study.

Chapter 2- Literature Review: Explores past research that studies the mechanical and economic benefits of Preflex beams and SFRC. Discusses how Preflex SFRC encased beams enhance current design methods in structural engineering.

Chapter 3-Material Properties: Discusses the process of creating a SFRC mix design and performing ASTM standard compression, tension, and modulus of rupture tests to determine material properties.

Chapter 4-Finite Element Modeling-Describes the modern development of FEM and the steps to model an SFRC Encased Steel Composite Beam in ABAQUS.

Chapter 5- Numerical Analysis: Compares the load-displacement curve of the experiment to the FEA results. Load-displacement curves for each parametric study are also given to determine the benefits of SFRC and preflexing.

Chapter 6- Summary and Conclusion: Draws conclusions on how the objectives of this research are met. It also provides further recommendations for this research and the overall benefits of Preflex SFRC Encased Steel Joist Composite Beams.

Chapter 2

Literature Review

2.1 Steel Fibers in Concrete

2.1.1 Advantages of SFRC

Research on steel fiber reinforced concrete (SFRC) started expanding in the1960's. SFRC is in popular demand because it can be used for high-rise buildings to reduce obstructive columns, long span bridges, and other engineering demands [17]. Steel fibers in concrete can help reduce multiple factors including early damage in structural members, maintenance, and overall construction costs.

SFRC is an extremely advantageous innovation in structural engineering that can help strengthen the weaker mechanical properties of concrete. Some of the benefits include but are not limited to; increased modulus of rupture and ductility, reduction in crack propagation, and less construction costs and labor [11]. Steel is a lightweight material with a higher carrying capacity than concrete [12]. Typically, normal concrete tends to be very brittle and not as ductile as steel. The low tensile strength in concrete allows the formation of "micro cracks" [14]. Concrete typically has a lower modulus of rupture (f_r). Therefore, concrete begins to crack more rapidly than steel, causing flexural failure. ACI code, chapters 6 and 13, give the requirements for longitudinal and transverse reinforcement (rebar and or stirrups) to prevent flexural and shear failure in load bearing members such as beams, columns, and slabs [3]. Steel rebar in concrete increases the flexural strength but does not alter the material properties of the concrete itself. Steel fibers can be added to concrete during mix design in order to create a hybrid material that performs well in compression and tension. These fibers can resist the development of more cracks due to their residual strength, which is a property not found in normal damaged concrete [16]. Figure 1 shows the difference in crack propagation between continuous concrete reinforcement and discrete reinforcement.

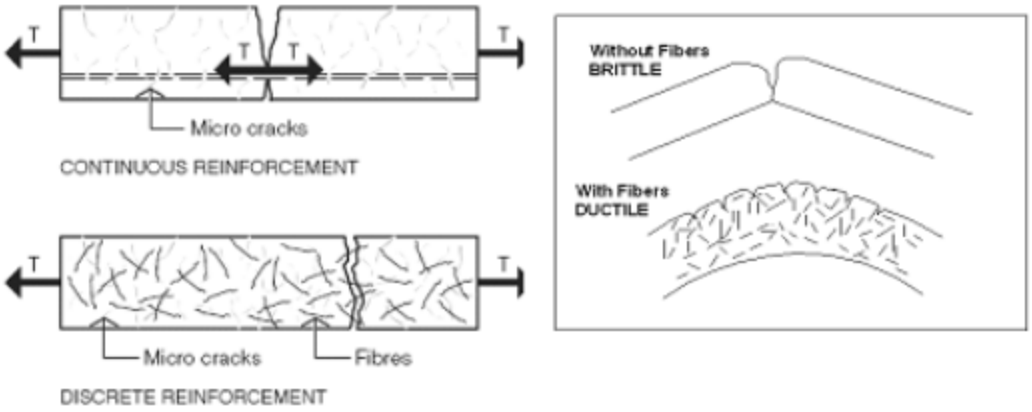

Figure 1.Steel Fibers in Concrete [11]

Although steel fibers are beneficial, the percentage of steel fibers added to the mix is important in order to maintain workability of concrete. This percentage depends on the total volume of the concrete or the "volume fraction" (V_f). The aspect ratio (l/d) is also important and is found by dividing fiber length (l) by its diameter (d) [11]. The physical characteristics of the steel fibers influence the concrete's performance. A higher aspect ratio means an increase in the fibers ability to resist flexure and a higher stiffness. When analyzing a high fiber concentration with long fibers there is an increase in flexural behavior because the bond stress improves the concrete [16]. Experiments have been done to test how the increase in the volume fraction affects the critical properties in the concrete. By increasing the V_f, the compressive strength, tensile strength, and modulus of rupture should increase significantly [11]. Adding fibers reduces the concern of shrinkage, but if the V_f is over 1.5% the workability of the concrete mix will decrease.

2.1.2 High Strength Concrete and SFRC

Some uses for advanced concrete materials such as SFRC are High Strength Concrete (HSC). HSC improves load bearing structural members such as lower floor columns of high-rise structures and shear walls. It is also common for long span bridges because it reduces the dead load of the bridge girders to create a large underpass [20]. ACI defines HSC as concrete with a 28 day compressive strength greater than 6000 psi. This is a greater strength than normal strength concrete. Improvements to normal concrete that create HSC involves varying the proportions of cement, water, aggregates, and certain admixtures.

The size of the aggregate can affect the bond between the cement paste, which will come into play during cracking. Certain admixtures are known for enhancing the strength of concrete when added to the mix design. The most common admixtures are Pozzolans such as fly ash and silica fume. These minerals increase the strength by reacting with the cement to create a C-S-H gel which improves the bond strength of the paste. Another common practice is to add a superplasticizer with a water reducing retarder. This increases the workability of the concrete and reduces the absorption of moisture of the cement.

Adding steel fibers to HSC can create an ultra-high-performance concrete with a greater compressive strength than 6000 psi. Research done by P.S. Song and S. Hwang studied the “mechanical properties of high strength steel fiber reinforced concrete” [20]. Steel fibers were added by volume fractions from 0.5% to 2.0%. The compressive strength of the SFRC reached a maximum strength at 1.5%. The concrete had a compressive strength 15.3% greater than the HSC. The Modulus of rupture increased by 126.6% at a volume fraction of 2.0% [20]. This increase in the physical properties of the concrete can improve the typical construction of HSC structures and further the development of SFRC.

2.2 Preflex Beams

2.2.1 Prestress vs. Preflex

Concrete alone does not perform well under high tensile stress. Due to this disadvantage, many methods have been developed to combat the flexural failure that leads to cracking in concrete. Prestress precast reinforced concrete beams became common in 1938 [20]. This method is applied by applying tensions to the rebar and then applying prestress forces so that the beam can have an upward deflection. Prestressed Concrete introduces stress to the member in locations where it will experience high tensile stress and counter act it as shown in Figure 2.

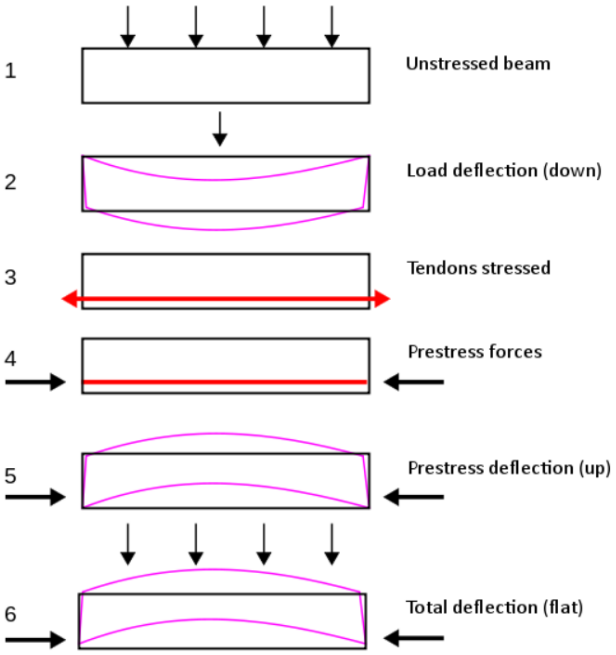

Figure 2. Prestressed Reinforced Concrete

Preflexing is a similar concept to prestressed concrete with the focus on introducing the flexure loads to a steel joist instead of tensioning the rebar. This innovation can be used with the combinations of concrete encased steel beams to provide a member that performs well under both compression and is controlled in tension. Numerical analysis comparing common bridge pre-stress girders and preflex girders show that preflex performs better [20]. Around the 1950s Preflex technology to provide camber to a concrete beam improved the construction of buildings and bridges [18]. The Preflex composite beam is fabricated with preflex loads to create the camber and then concrete is cast over the flange. This preflex beam is transported to the construction site [20]. The process of preflexing is done by applying an upwards force over the span of the beam using propping and jacking systems [4]. After the concentrated loads are applied the load remains on the beam according to the amount of deflect desired for the beam. These loads should be the maximum capacity of the beam, and then the deflection will reflect the amount of deformation that the designer is hoping to prevent [4]. Once the beams have been loaded concrete is cast according to encasement design around the steel girder. Now the beam can be assumed to be in compression [9]. Once the concrete hardens the loads are removed and then the beam returns to its original shape. The construction of preflex members can be seen in Figure 3.

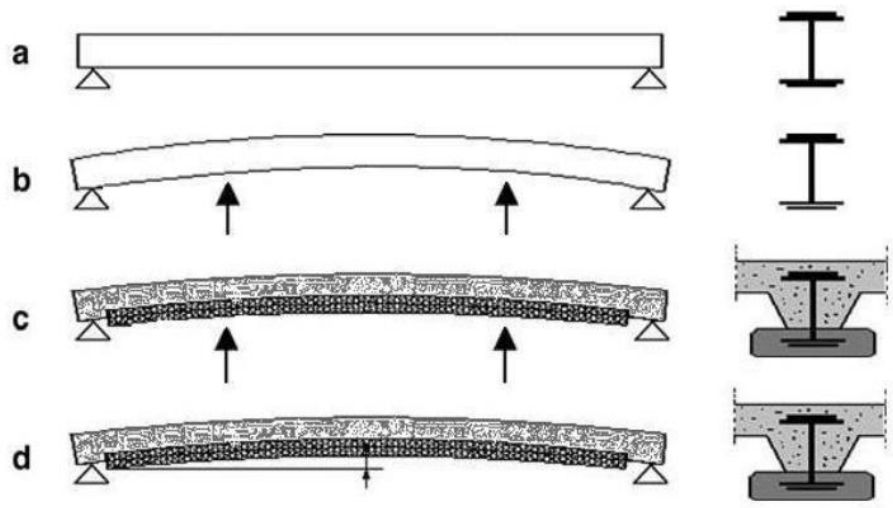

Figure 3.Preflex Beam Construction Stages [9]

A study by Hegger and Goralski explores with the benefits of steel beams encased with normal concrete [13]. Shear connectors and additional longitudinal reinforcement are used for this specimen. The encased steel section attaches to a slab to form an assembly. Figure 4 shows the cross section view of one of the beam-slab assemblies. These beams are placed under two concentrated loads to determine the moment capacity.

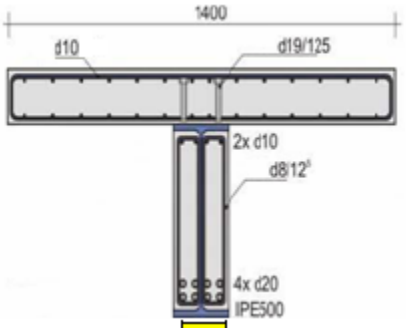

Figure 4. Cross Section of Encased Steel Beam [9].

This moment-rotation results from Hegger and Goralski experiment are re-analyzed using FEM in a separate study, “Nonlinear Analyses of Composite Preflex Steel Beams Encased in Concrete” [9]. This study uses the same properties and dimensions of the experimental specimens and models the specimen in a FEM software called ANSYS. Load-deflection and moment-rotation curves are given from this software

and compared to the experiment's moment-rotation curves. The FEA study also investigates the benefits of preflexing the steel section to see if the ultimate moment capacity of the composite encased beam increases. After the values are provided for the moment-rotation curves, the three categories; experimental, straight-beam (numerical), and preflex-beam results are compared. Figure 5 shows the moment-rotation curve for the FEA of an encased beam-slab assembly.

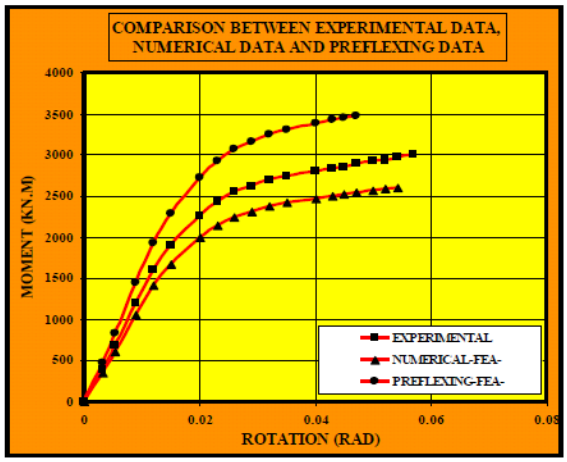

Figure 5. Moment-Rotation Curve with FEA [9].

From Figure 5, the preflex beam has a higher moment capacity than the straight beam. For the Numerical (straight beam) analysis the maximum moment was 2595 kN-m (22,967 kip-in) but when preflexed it becomes 3473.78 kN-m (30,738 kip-in) [9]. This is the anticipated result because as a beam is preflexed, the flexural capacity increases.

2.2.2 Preflex Beams in Long Span Bridges

Long span bridges tend to fail under progressive collapse where adjoining structural members collapse after the primary member fails. Single loading events cause failure when a certain region of the bridge is prone to single point vulnerability [22]. After the Ronan Point collapse in England in 1968, and terrorist attacks such as the World trade Center on September 11th, 2001, design codes that prevent progressive collapse became a major focus [22]. Long span bridges composed of either steel or concrete are susceptible to single point vulnerability and need to be designed against it. From AASHTO LRFD section 6 on Steel Girders:

"The criteria for a refined analysis is used to demonstrate that part of the structure is non-fracture critical has not yet been codified. Therefore, the loading cases to be studied, the location of potential cracks, degree to which the dynamic effects associated with a fracture are included in the analysis, and the fineness of the models and choice of element type should be agreed upon by the Owner and the Engineer.." [1]

This statement shows that more research is needed to improve code for the points in bridges where there is intense cracking. On method of improvement may be the combinations of concrete and steel, which are both used as girders in long span bridges. Preflex SFRC Encased Steel Joist Composite Beams can postpone the progressive collapse by increasing the ductility of the members and postponing the crack propagation.

There is also a need for FEA of bridge research using fiber reinforced beams, so that AASHTO specifications can improve. The benefits of using a beam with fibers is the reduction of corrosion in the beam that is found often in AASHTO specified reinforced beams. With the use of polymer, steel, or other types of fiber this issue can be reduced. AASHTO has recently released new specifications for concrete bridges beams prestressed with Carbon Fiber Reinforced Polymer (CFRP) systems [12]. The research investigates the flexural behavior, strain response, and load capacity of a controlled I-beam and a bridge model. Carbon Fiber Composite Cable (CFCC) strands are prestressed into the I-beams and bridge model and tested using ACI 440.4 design guidelines and the Unified Design Approach. After testing the ultimate load-carrying capacity of the CFRP specimens were close to the expected experimental values. The CFCC strands are not damaged after failure of the beam or the bridge model and experienced 66.7% of the ultimate strain. [12]. More investigation into this area of FEM bridge research is needed.

Another advantage in preflex bridges is that the slab increases in bending capacity and stiffness because of the preflex girders. The flange of the steel can handle pre compression stress better which reduces cracking [23]. There is less deflection in the lower part of the concrete beam due to extra flexural stiffness. Certain types of bridges like railway bridges require girders able to carry heavy loads. Prestressed girders are often used for these structures, but the technology of preflex beams can improve the quality of these bridges. Research has been done on a precast prestressed concrete and bridge model versus a preflex steel beam with a concrete flange bridge model [23]. The results shows that a preflex bridge girders

performs better than the precast, prestressed bridge girders. The preflex superstructure is lighter and deflects less under the same load as the prestressed [23].

2.3 SFRC Encased Steel Joist Composite Beams

Composite or hybrid structures have had a lot more research studies recently due to the structural benefits they bring. By combining different types of materials, the overall properties of a member become enhanced [15]. For this study the beneficial properties of concrete and steel come together in both a composite and hybrid manner to create a member with strong compressive strength and increased tensile strength. Some of the other properties that benefit from using a composite system of concrete and steel are inherent mass, stiffness, damping, speed of construction, and the economical factor. It is more cost efficient to use a lighter weight steel member encased with reinforced concrete [15]. Steel beams are known for being able to handle flexure well but are prone to buckling under compression. Encasing a steel beam with concrete can prevent buckling so the steel can withstand the load [15]. Fire and corrosion are common issues when steel beams are used independently. Since concrete has a slow rate of heat transfer, combining it to steel eliminates this issue [15].

The mechanics of an encased steel beam considers the elastic performance of the hybrid member. Yield stress of the member is dependent on the steel joist that is being encased. When the tensile strength is greater than the concrete's ability, this is where cracks will develop [15]. The stress and strain curves for an encased beam can be seen in Figure 6.

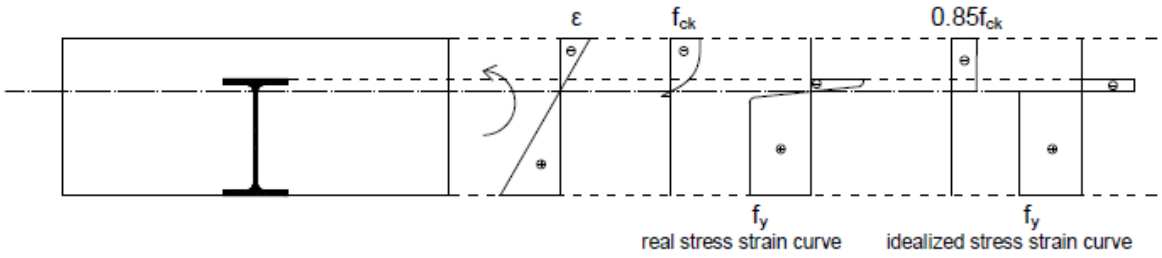

Figure 6.Stress Strain Curve for Encased Beam [15]

Another mechanical feature to consider is the flexural rigidity of a composite member. Since the member is composed of two materials, it has variable rigidity. The deflection depends on this rigidity especially for longitudinally encased beams [15].

Steel fibers inside concrete have shown in past studies to increase the strength and ductility and reduces spalling in the concrete [14]. The available experiment research, “Experimental Study of FRC-Encased Steel Joist Composite Beams”, investigates steel fiber behavior with straight beams [14]. A beam to column design using this concept can be seen in the research done by Khuntia and Goel, in Figure 7 [14]. This sub assemblage design reduces the need for shear connectors, longitudinal, or transverse reinforcement is setup so that members are connected by steel to steel. This way the whole system can be designed using cast-in-place or precast construction [14].

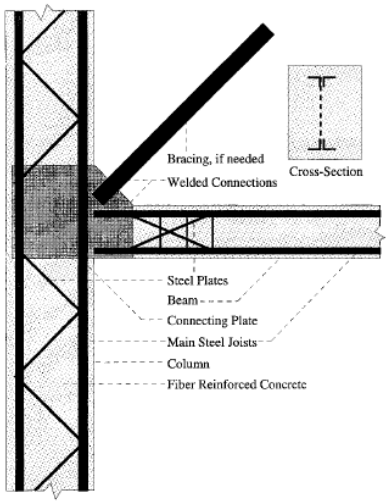

Figure 7. Subassemblage of Steel Encased in FRC [11]

Khuntia and Goel’s experiment focuses on testing steel joists encased with fiber reinforced concrete with 1% of steel fibers inside [14]. This test uses monotonic loading on the beam to compare the amount of load the beam can handle and the mode of failure. Loading is done by an actuator that goes up to 490 kN (110 kips). The actuator is placed at the center of the beam and the crack patterns are measured. The beam showed ductile behavior and reached a load capacity of 120 kN (27 kips) [14]. The SFRC was strong enough to withstand the applied shear before it reached the steel section. The crack patterns can be seen

in Figure 8. Other specimens were tested to determine how different type of steel joists could increase the flexural capacity of the composite beam.

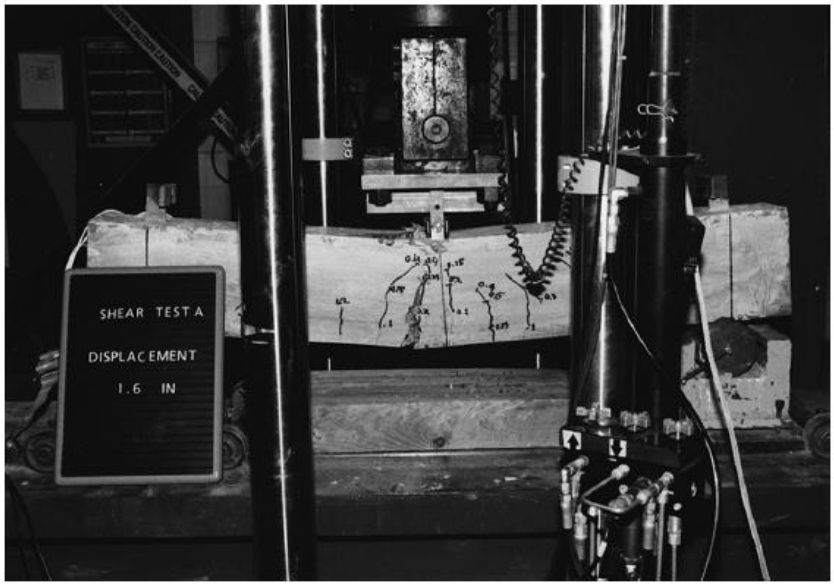

Figure 8. Crack Pattern of Specimen A [14]

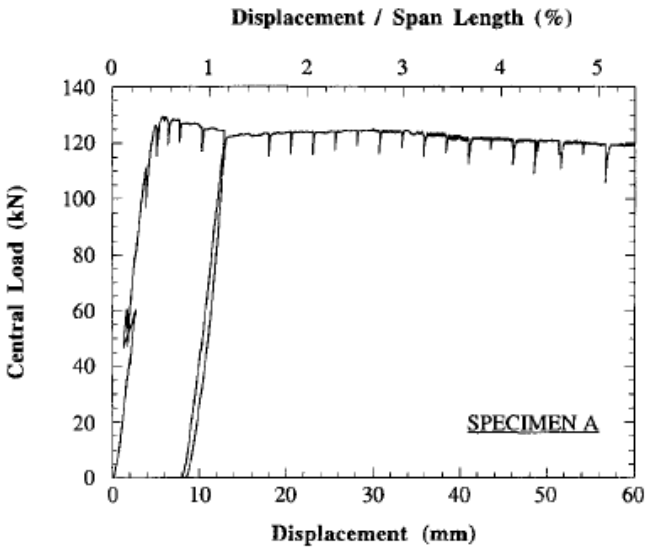

Figure 9.Load Displacement Curve of Specimen A [14]

From the load displacement curve seen in Figure 9, the conclusion is that the SFRC-encased open-web steel joist beam had great strength and ductility. This experiment shows that steel fibers help make a

encased beam stronger than if a typical reinforced concrete member using just rebar to increase tensile strength. Flexural capacity increases due to the steel fibers, but more can be done to improve the composite beam. By utilizing the composite beam design with preflexing, a stronger more ductile member can be used in today's structural engineering designs. The dimensions used to create the specimen and the load steps used can be input into finite element software to determine if FEA can produce similar results.

Chapter 3

Material Properties

3.1 Concrete Mix Design

Before performing the numerical analysis using SFRC, the material properties are found through lab testing based on ASTM C192/C192M procedure [7]. The first step is to create a concrete mixture in the lab and add the volume fraction, V_f, of steel fibers. In order to do this the following materials must go into the mix for a 27 cf batch; coarse aggregate, fine aggregate, cement, and water. The mixture quantities are shown in Tables 1 through 3 and the type of steel fibers used is seen in Figure 10.

Table 1. Material Properties for Concrete Mix

	Cement	Fine Aggregate	Coarse Aggregate
Specific Gravity	3.15	2.82	2.5
Density (lb/ cf)	196	176	160.68
Fineness Modulus		2.98	
Dry Rodded Wt (lb/cf)			99.2
Absorption Capacity (%)		0.8	2.5
Moisture Content (%)		0.13	1.1

Table 2. Mix Proportions for 27cf Batch

Materials	SSD (lbs.)	Moisture Correction (lbs.)	Mix Proportions (lbs.)
Cement	680	n/a	680
Coarse Aggregate	1263	17	1246
Fine Aggregate	1752	12	1741
Water	306	29	335
TOTAL	4001		4001

Table 3. Material Properties of Steel Fibers

Length (in)	Diameter (in)	Tensile Strength (ksi)
1.3	0.02	174

Figure 10.10. Steel Fibers [9]

The mixing process is done in a standard lab concrete mixer in the Civil Engineering Laboratory Building at The University of Texas at Arlington. There are three volume fractions of steel fibers in each concrete batch. The first batch has 0% V_f steel fibers, the second has 0.5%, and the third has 1%. After the concrete is made in the mixer it is immediately put into the molds that ASTM specifies for each type of test [7]. The concrete molds for the compression test are nine cylinders of 4" x 8". The next nine molds are the rectangular beams that are 6" x 6" x 20" for the modulus of rupture test. The last set of nine molds are for the cylinders that are 6" x 12" for the split test. Dry rodding helps consolidate the mix into the molds and for this process is important in order to ensure that the gaps created from the steel fibers do not remain once in the mold. Figures 11-13 show each SFRC mix design in the molds that will be tested.

Figure 11. 0% SFRC in Beam and Cylinder Molds

Figure 12. 0.5% SFRC in Beam and Cylinder Molds

Figure 13. 1% SFRC Batch in Beam and Cylinder Molds

A slump test is done for the 0.5% mix to determine workability and consistency. From Figure 14 the slump test shows the mix has a 1” slump.

Figure 14. Slump Test on 0.5% Concrete Mix

Figures 15- 22 show the cylinders and beams placed in the humidity-controlled room. Each V_f of steel fibers can be seen from red label markings. The textures of the concrete for each batch are very different depending on the percentage of steel fibers. The 0% concrete beams and cylinders have a much smoother surface. In the 0.5% and 1% beams and cylinders this is not the case. Instead they appear much more jagged and more porous since the fibers are drying into the concrete. This is because when the steel fibers mix into the concrete there are two elements to combining, making the mix less consolidated and porous.

Figure 15.Humidity Controlled Room

Figure 16. 4" x 8" Cylinders for Compression Test

Figure 17. 0.5% Cylinders (4" x 8")

Figure 18. 1% SFRC Cylinders (4" x 8")

Figure 19. Cylinders for Split Test (6" x 12")

Figure 20. 0% SFRC Beams (6”x6”x20”)

Figure 21. 0.5% SFRC Beams (6”x6”x20”)

Figure 22. 1% SFRC Beams (6”x6”x20”)

3.2 Compression, Split, and Modulus of Rupture Tests

3.2.1 Compression Test

Once the beams are ready for testing, ASTM C39 provides the method for testing the small cylinders (4" x 8") [5]. A computer-controlled compression machine from the Civil Engineering Lab Building is used. The cylinder is placed where its circular cross section is directly in contact with the load. The process is done by a consistent incremental loading of 400 lbs/sec until the cylinder reaches its ultimate load capacity. Figure 23 shows the machine used for testing.

Figure 23. Compression Test Machine

This load is used to calculate the compressive strength which can be found in Equation 1 where f_c' is the compressive strength, P represents the load capacity, and r is the radius of the cylinder. The elastic modulus of concrete can be found from Equation 2. Sample calculations for compressive strength and elastic modulus can be found in Appendix A. Figures 24- 29 shows the setup of each compression test and the point of failure.

$$f_c' = \frac{P}{\pi r^2} \qquad (Eq. 1)$$

$$E_c = 57000 \times \sqrt{f_c'} \qquad (Eq. 2)$$

Figure 24. 0% Cylinder (4” x 8”) Compression Test Setup

Figure 25. 0% Cylinder collapses at 36 kips

Figure 26. 0.5% Cylinder (4” x 8”) Compression Test Setup

Figure 27.0.5% Cylinder collapses at 48 kips

Figure 28. 0.5% Cylinder (4” x 8”) Compression Test Setup

Figure 29. 1% Cylinder collapses at 53 kips

When comparing each cylinder, the 0%-cylinder from Figure 25 has significant fractures and cracks at an average of 36 kips. The uniaxial compression forms micro cracks very early on, which over time expand in the same direction as the stress. In the 0.5%-cylinder, the steel fibers prove effective by maintaining the bond between the cracks and has a load capacity of 48 kips. The cracks shown in Figure 27 do not extend to the bottom, meaning although the cylinder reaches maximum load capacity, it is still able to resist pullout force on the steel fibers in some regions. The 1% fiber collapses at the largest load capacity of 53 kips, and it does not show significant fracturing like the other specimens as seen in Figure 29. The cracks propagate around the bottom and top of the cylinder, but the center remains intact from the steel fiber bond.

3.2.2 Split Test

Split tests are done according to ASTM C496 using 6" x 12" cylinders [8]. The beam lies horizontally on the testing table as a diametral compressive force loads it along its length. The machine applies load at a rate of 100 lb/sec till the cylinder reaches failure along the vertical diameter. A steel plate with side plates is placed around the beam during this process to reduce the amount of compressive stress where the load will be applied. Once the ultimate load is recorded, the tensile strength is calculated according to Equation 3. Ft is the tensile strength, P is the load capacity, L represents length, and D is the diameter of the cylinder. Sample Calculations for tensile strength can be found in Appendix A.

$$f_t = \frac{2P}{\pi LD} \qquad (Eq. 3)$$

Figure 30. Split Tensile Setup

Figure 31. 0% SFRC Split Test

For the split test in Figures 30 and 31, of the 0% large cylinder, the specimen broke at an average of 25 kips. For the 0.5% cylinder, the specimen broke at 36 kips, and at 1% the cylinder broke at 41 kips.

3.2.3 Modulus of Rupture Test

Flexure tests are done using a rectangular beam (6”x6”x20”) as per ASTM C78, and placed length wise under the machine [6]. Loading will occur at the 1/3 points on the beam in order to exhibit pure bending in the middle portion. This specimen is loaded at 50 lb/sec and fracture stress occurs in this middle portion called modulus of rupture. The machine records the ultimate load capacity and Equation 4 is used to find the modulus of rupture, f_r. P is the load at failure, L is the length of the beam, D represents the depth, and B the width. Sample calculations for the modulus of rupture can be found in Appendix A. Figures 32-37 show the setup and testing of 3 beams to determine the modulus of rupture.

$$fr = \frac{PL}{BD^2} \qquad (Eq. 4)$$

In comparison, Figures 33 and 35, show the improvement in flexural strength of the concrete when 0.5% volume steel fibers are added. In Figure 33 the beam cracks along the entire midspan section at a load of 6.6 kips. Once the steel fibers are in the concrete, the beam appears to harden like the 0% but performs better in flexure. This beam reaches its capacity at 7.5 kips, which shows that the beam is improving with the addition of steel fibers. The cracking stops midway at the beam and does not fully collapse the beam.

The 1% SFRC beam fails at 9 kips, which shows that adding steel fibers into a normal concrete mix can improve the modulus of rupture of a beam.

Figure 32. 0% SFRC Beam-Modulus of Rupture Setup

Figure 33. 0% SFRC Beam at Failure Load 6.6 kips

Figure 34 0.5% SFRC Beam-Modulus of Rupture Setup

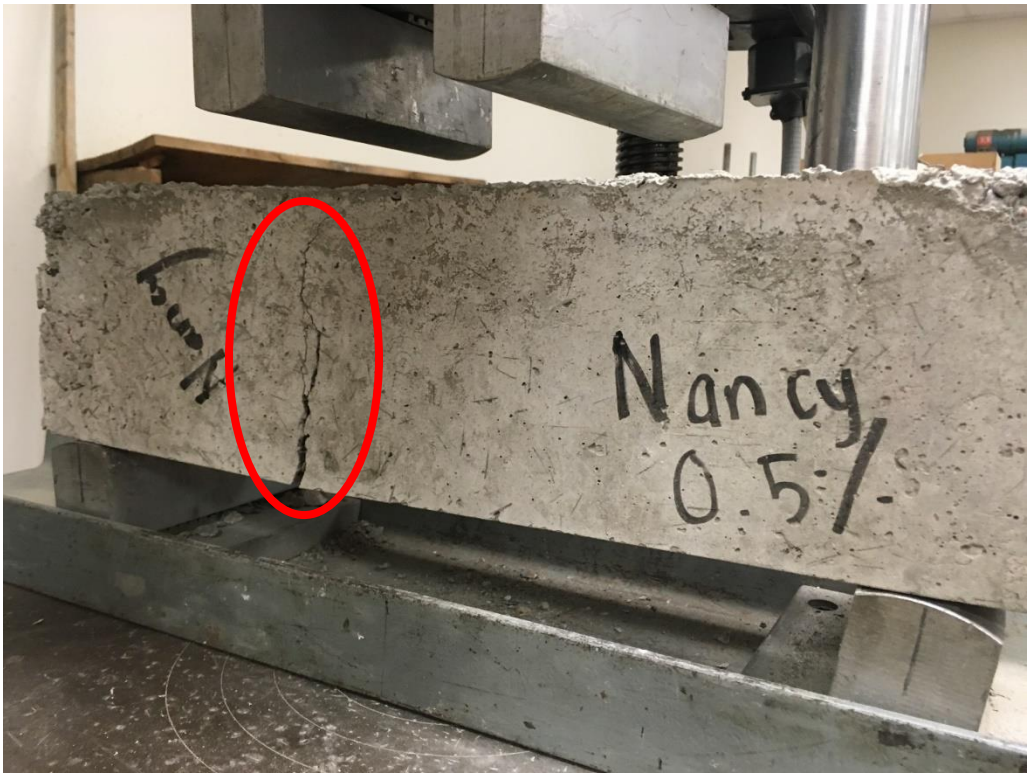

Figure 35.0% SFRC Beam at Failure Load 7.4 kips

Figure 36. 1% SFRC Beam-Modulus of Rupture Test Setup

Figure 37. 1% SFRC Beam at Failure Load is 8.7 kips

3.2.4 SFRC Material Properties

Tables 4 through 6 summarize the compressive, tensile, and modulus of rupture values found from the SFRC material lab testing.

Table 4. Concrete Compression Test

Concrete Compression Strength, f_c' (psi)			
Fiber Volume (%)	0	0.5	1
Small Cylinder 1	2810.51	3732.484	4219.745
Small Cylinder 2	2945.86	3933.121	4335.191
Small Cylinder 3	2878.185	3832.803	4277.468
Average f_c' (psi)	**2878**	**3832**	**4277**

Concrete's compressive strength, f_c', determines its ability to uniaxial loading. Table 4 shows that as the volume of fibers increases, so does the compressive strength. Steel fibers create a bond inside the concrete that postpones buckling and reduces cracking.

Table 5. Concrete Split Test

Concrete Tensile Strength, f_t (psi)			
Fiber Volume (%)	0	0.5	1
Cylinder 1	214	324	331
Cylinder 2	232	365	530
Cylinder 3	223	290	585
Average f_t (psi)	**223**	**315**	**557**

Note: For the "1%-Cylinder 1" specimen, this value is ignored in the Average f_t value for 1% SFRC, due to inconsistency in testing.

The change in concrete's tensile strength capacity can be seen from Table 5. The addition of fibers into the concrete mix, increases the tensile strength of concrete by almost 400 psi.

Table 6. Concrete Modulus of Rupture Test

Concrete Modulus of Rupture, f_r (psi)			
Fiber Volume (%)	0	0.5	1
Beam 1	617	856	732
Beam 2	565	648	861
Beam 3	648	556	811
Average f_r (psi)	**609**	**686**	**801**

By the addition of steel fibers, concrete's modulus of rupture increases significantly. As seen from Table 6, f_r for 1% volume of steel fibers addition is around 800 psi. This mechanical property can be increased if more steel fibers are added. Other factors should be considered when adding steel fibers, but the material properties prove that the beam should perform well under flexural stress because the steel is postponing micro cracks from forming.

3.2.5 Angle Steel Properties

The properties for the angle steel sections can be seen in Table 7. These properties come from the available experiment in order to compare each beam analysis.

Table 7. Angle Steel Section Properties

Angle Steel Section	Yield Strength, Fy (ksi)	Ultimate Strength Fu (ksi)	Elastic Modulus, Es (ksi)
1.5" x 1.5" x 3/16"	36	73	29000

Chapter 4

Finite Element Modeling in ABAQUS

4.1 General

Finite Element Method (FEM) analysis is the numerical approach to complicated problems such as the modeling of an element with different materials and dividing into smaller elements to perform analysis. This concept uses many algebraic equations to find the most approximate solution for problems and yield an accurate representation of the results. This research focuses on analyzing a SFRC encased steel joist composite beam using a FEA tool called ABAQUS. ABAQUS is a Computer-Aided-Engineering software that helps model and perform tests on components to determine its various static and dynamic properties. This study investigates how FEA can confirm the results of an experiment "Experimental Study FRC-Encased Steel Joist Composite Beams" by Khuntia and Goel [11]. The experiment takes two angle steel joists and encases it in 1% SFRC and performs a load analysis using an actuator. These experimental results provide the amount of midspan displacement under monotonic loading. The same "Experiment Specimen" is modeled in ABAQUS under monotonic load analysis to achieve the same results of load-midspan displacement. A second part of the FEA are two parametric studies. While using the same dimensions of the Experiment Specimen, there are two models made in ABAQUS. The first model is a straight beam model with the parametric study parameters (PSP) for f_c and f_r for 0%, 0.5%, and 1% SFRC. The second study models a preflex beam with the same PSP values as the first model. The purpose of modeling and analyzing two different beams in ABAQUS is to see how the load-displacement relationship improves for different parameters.

4.2 FEA in Civil Engineering

4.2.1 Progression of FEA

The application of the FEM was created and popularized by collaborative and individual researchers. The evolution of FEA into engineering required the use of matrix structural analysis, variational approximation, and the computer [19]. There are many approaches and advantages of this method, but the main purpose is to take any geometrical object and divide it into smaller elements to combine the solution of the elements by variational approximation. Four of the well konwn pioneers involved in the development of computational mechanics that started in aeronautical engineering are John H. Argyris, Ray W. Clough, M.J. Turner, and

O.C. Zienkeiwica. These engineers computerized FEM and made it applicable to different fields of engineering. Computerized FEM began in the 1950s when Turner used the Direct Stiffness Method to create the first continuum based finite element for the aerospace industry [19]. Various components were added by other engineers such as; isoparametric modeling, shape functions, and the Rayleigh-Ritz link to the energy principle [19]. This computerized mathematical model could assemble 2D plate elements and create an in-plane stiffness matrix for different shapes such as rectangles and triangles. When analyzing a low order of elements, the solution does not exhibit the realistic engineering values desired [19]. By increasing the number of elements, the solution is improved. This process is considered the refinement of the mesh or the “mesh convergence” [10].

Original analysis was performed on small structures specific to the aircraft industry. The structural analysis method used before was the Classical Force Method which took an element as a transducer of forces to develop stiffness equations from flux assumptions [19]. Each of the engineers mentioned had a part in introducing FEA for various usages. Argyris is responsible for performing the first “displacement-assumed” finite element. By the 1960s, Clough made the connection of computerized FEA to Civil Engineering problems. Clough took the approach to Berkely where the first research of FEA in Civil Engineering was done. Zienkiewicz also progressed the Civil Engineering field by writing one of the first textbooks so others could learn about FEA [19]. From then onwards the work that had begun with airplane structural analysis was introduced to various industries where the study of discrete elements could improve field related problems.

4.2.2 Application of FEM in ABAQUS

Many fields use FEA to solve mathematical problems with a plethora of functions, parameters, and potential solutions. FEA development can now help Civil Engineers perform analyses such as finding small strains, displacements, and the elasticity under static and dynamic loads. In order to reduce the amount of work done by hand or experiments, FEA software takes these same problems and uses computer programming to create a matrix of equations to formulate approximate solutions. For this research ABAQUS is the FEA software that models and analyzes the beam to find load-displacement under a static load. It does so by

discretizing it into finer elements and formulating a solution from the given parameters and controlled variables.

ABAQUS/CAE (Controlled ABAQUS Environment) is an interactive environment to make finite element models and perform analyses. The components of an ABAQUS model are creating nodes and elements by discretizing geometry, section properties, material data, load and boundary conditions, analyses, and output requests [21]. ABAQUS can model and analyze the solutions for various fundamental concepts such as elastic, thermal, fluid dynamics, electrostatics etc. by taking the governing equation and applying the boundary conditions [2]. These analyses are performed through a set of simultaneous algebraic equations. Jobs monitor the analysis and the results are shown in 3D visualization for evaluation purposes. The equations used for basic analysis are from mechanics concepts and nonlinear finite element analysis. These equations set the requirements for finite rotations, deformation, stress, and strain [2]. Matrices are extremely important in calculating these variables, because there are a myriad of solutions and they need to be put into a matrix to organize the results for computer analysis. The governing equation that ABAQUS uses for a for elastic behavior concept comes from the Direct Stiffness Method which is the most common implementation of the FEM. This takes the stiffness of the member in a structure and forms a matrix relation to find the displacement. This general formula is shown in Figure 38.

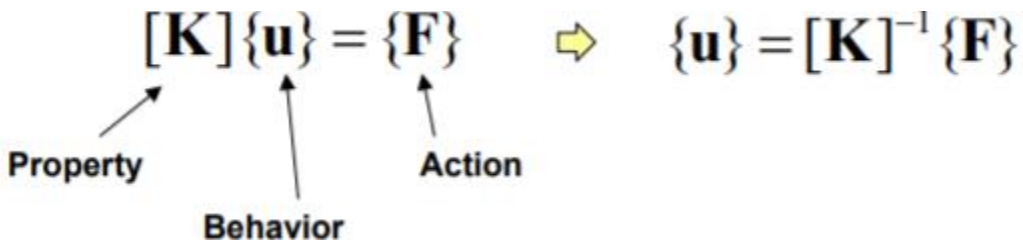

Figure 38. Fundamental Concept for Algebraic Equations in ABAQUS [21]

The variable “K” represents the Stiffness value, “u” represents the Displacement, and “F” represents the Force. In FEA the stiffness matrix is used for elastic behavior in order to analyze the displacement occurring at different nodes. In ABAQUS, the model is being discretized into thousands of nodes, so matrices are essential as is the concept of piecewise polynomial interpolation [21]. This connects the elements and interpolates over the entire structure to form a solution. For nonlinear analysis, the goal is to obtain a

convergent solution with minimal effort. Once the model is ready for analysis, ABAQUS allows two approaches for setting up the step increments that will load the model. The first approach is the Direct user control of the increment size allows the user to set a number for the increments within one step that the analysis can increase steadily for. The second approach is Automatic control where the user sets tolerances and error parameters for the steps [2].

FEA exists today to help in the numerous complex energy and mechanical functions of elements that are difficult to solve by hand. By applying the Direct Stiffness Method to a computerized method, a member can be discretized and analyzed at individual nodes. This provides an approximate solution for load displacement problems within a margin of error. Digital computation reduces a significant amount of time spent in labs trying to imitate the same results. Today software such as ANSYS, ABAQUS, FEA, Autodesk etc. can be used to solve the displacements, stresses, and more functions in different objects.

4.3 Modeling in ABAQUS

4.3.1 Creating Parts

The first step in ABAQUS is using the “Create Part” tool to model the geometry and regions of a SFRC encased steel joist composite beam. This tool models the dimensions and components for each part as seen in Figure 39. ABAQUS interface creates the part on a coordinate grid, so the lines reference to the coordinate points. If a portion of the member needs to be cut or perforated, the “Create: Cut Extrude” tool is used.

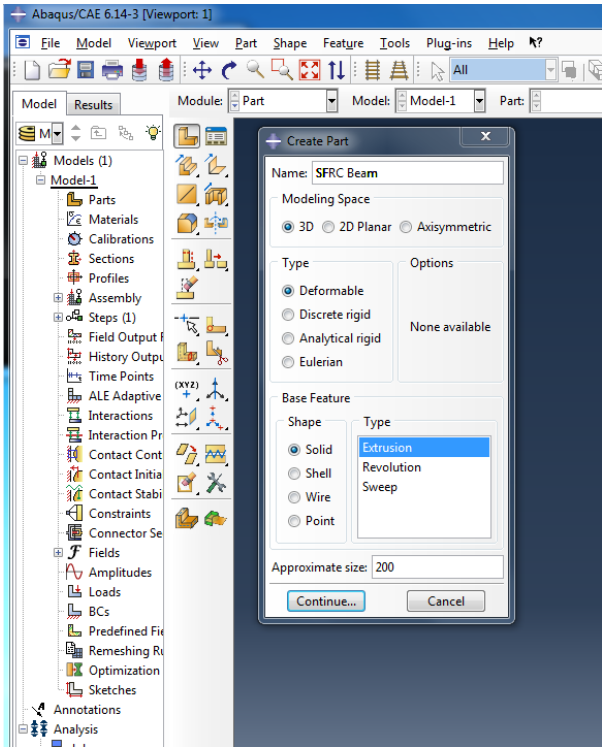

Figure 39. ABAQUS- Initial Step "Create Part"

4.3.1.1 Straight Beam Modeling

For this study, SFRC beam and angle steel beams are initially individual “Parts” in ABAQUS and then combine to form the SFRC encased steel joist composite beam. The process starts with modeling the SFRC component as a rectangular beam and then modeling the second component as two angle steel joists. The dimensions of the SFRC beam are 6 inches in width, 8 inches in height, with a span of 44 inches. The steel angles are 1.5 by 1.5 inches with a thickness of 3/16th inches. The angles also span 44 inches. These dimensions come from the composite beam in the available experiment, as seen in Figure 40 [11]. A summary of the dimensions for each component can be seen in Table 8. Modeling of each straight beam part before merging are shown in Figures 41-44.

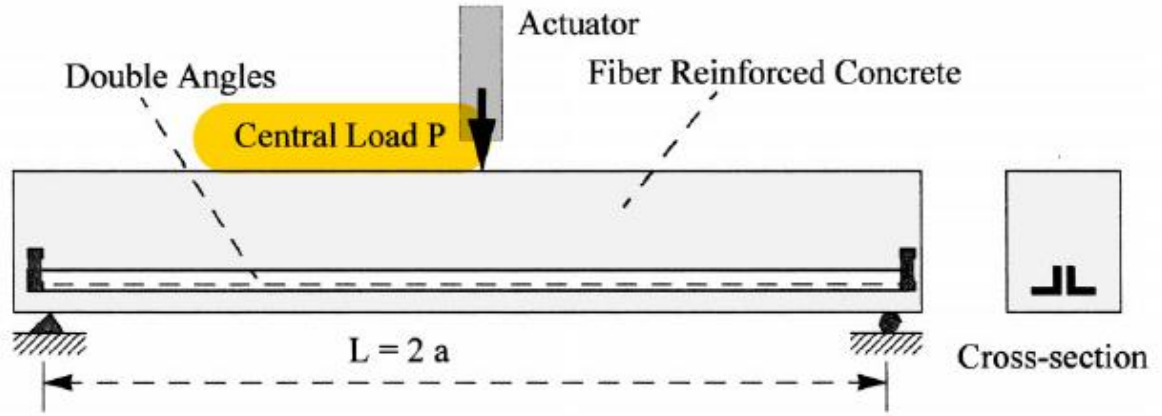

Figure 40. Design of SFRC Encased Steel Joist Composite Beam [11]

Table 8. Dimensions of SFRC and Angle Steel Parts

	Width, w (in)	Height, h (in)	Depth, d (in)
SFRC Beam	6	8	44
Angle Steel Joist (t=3/16")	1.5	1.5	44

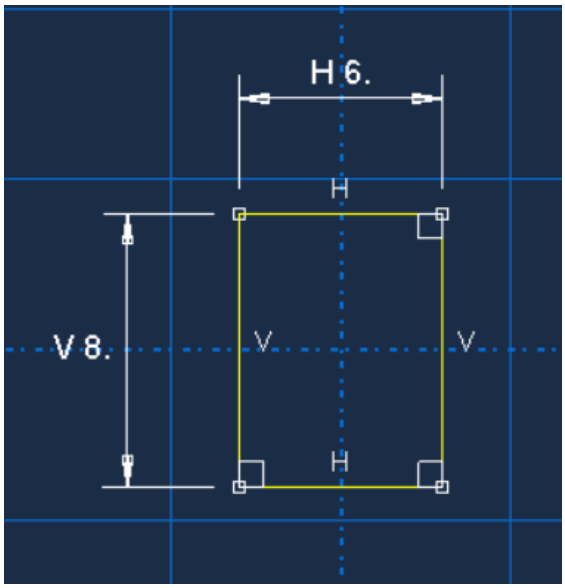

Figure 41.ABAQUS-SFRC Beam Cross Section (Units are inches)

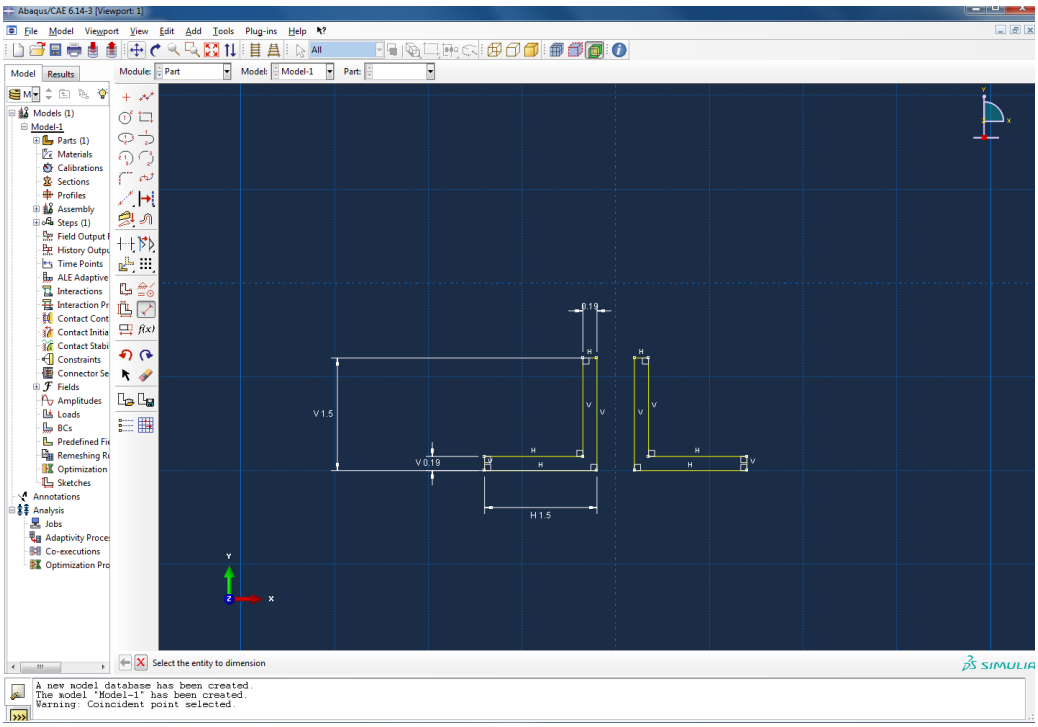

Figure 42. ABAQUS-Angle Steel Cross-Section (Units are inches)

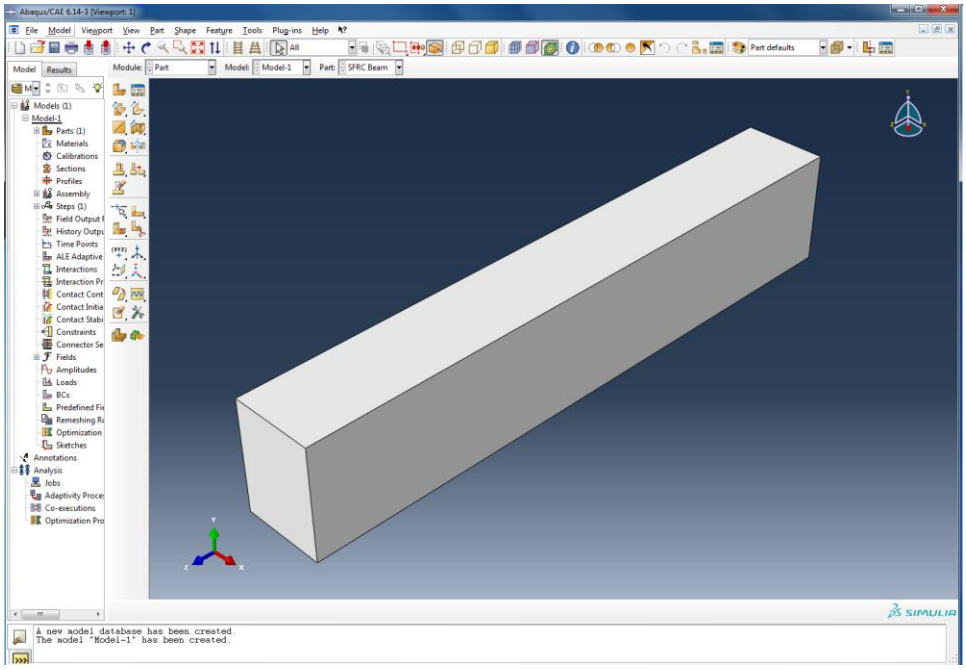

Figure 43. SFRC-Solid Shape

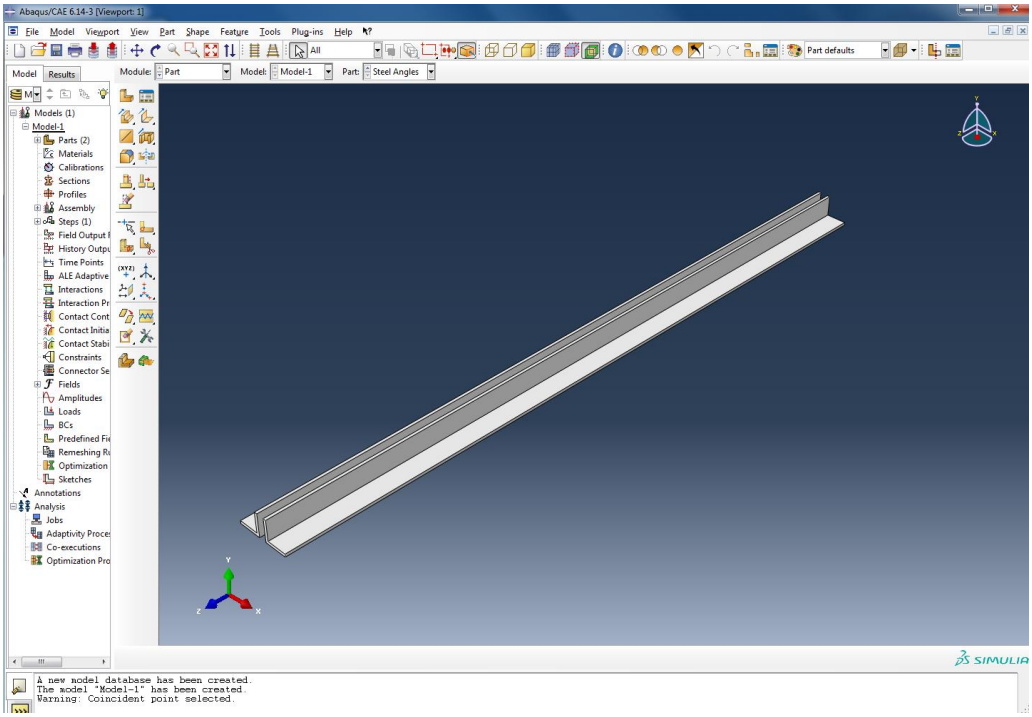

Figure 44. Angle Steel-Solid Shape

4.3.1.2 Preflex Beam Modeling

The preflex model has a camber that depends on the maximum deflection that the straight beam experiences. This amount of deflection is applied to each steel section. In construction the concrete encases around the preflex steel and take the same preflex shape after settling. Equations 5 through 8 determines the maximum deflection; bending moment, flexural stress, and load capacity for the preflex amount respectively. Calculations can be seen in Appendix A.

$$\Delta_p = \frac{PL^3}{48EI} \qquad (Eq.5)$$

$$M = \frac{PL}{4} \qquad (Eq.6)$$

$$\sigma = \frac{My}{I} \qquad (Eq.7)$$

$$P = \frac{4\sigma I}{Ly} \qquad (Eq.8)$$

The ultimate load for the steel itself is 1600 pounds, which provides a maximum displacement of .45 inches. This displacement is the amount of camber in the preflex beam as shown in Figure 45.

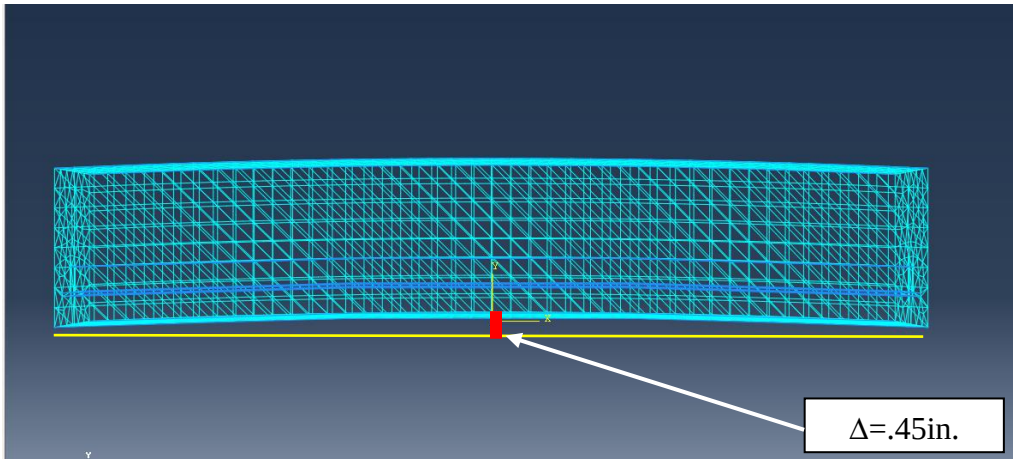

Figure 45. Preflex Beam

4.3.2 Meshing Components

A mesh is created on the beam in order to discretize the model and form nodes on the components where the load will be distributed. Refining the mesh gives more degrees of freedom in the critical areas where stress occurs while a coarse mesh should be designed in general areas where there is not a high amount of stress. Each type of mesh defines the cross section of the discretized finite elements. For a 1” x 1” mesh the finite element model generates about 20,000 elements with individual nodes in the model. In order to determine the ideal number of elements for this model, a mesh convergence is done in Chapter 5. When doing a refined mesh, the region can sometimes fail. Some of the reasons may be “inadequate seeding” or “bad geometry”. In this case the steel joist has small edges and faces that make the instance imprecise. ABAQUS recognizes this as bad geometry and the assembly needs to be meshed as a tetrahedral (triangular elements) instead of hexahedral (cubic elements) when choosing a refined mesh such as 1” by 1”. Figure 46 shows the meshed finite element model.

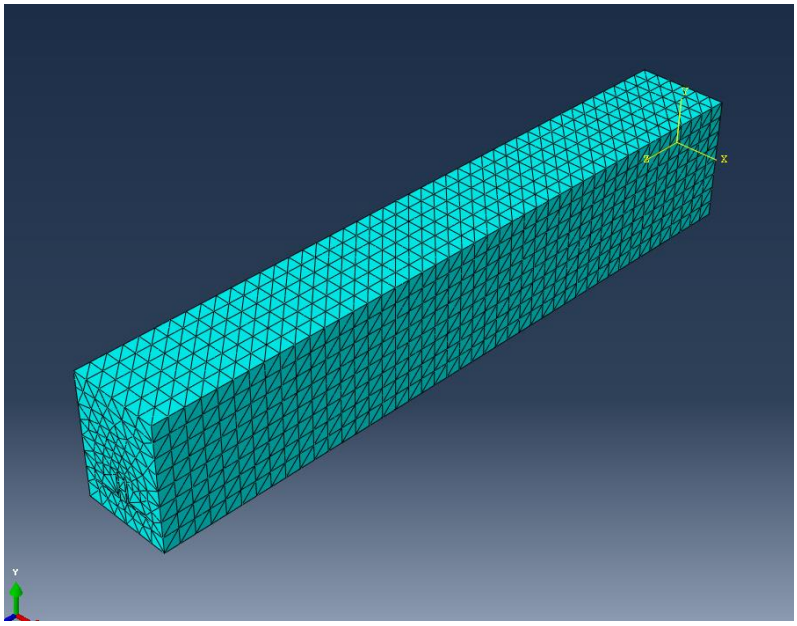

Figure 46. 1” x 1" Mesh

4.3.3 Material Properties

The values for the Experiment Specimen and the PSP are put into ABAQUS. For ABAQUS to perform the analysis for the created parts, the physical properties of the elements must be input into the “Material Manager” tool as shown in Figure 47. This tool defines the materials, sections, and assigns each section the parts.

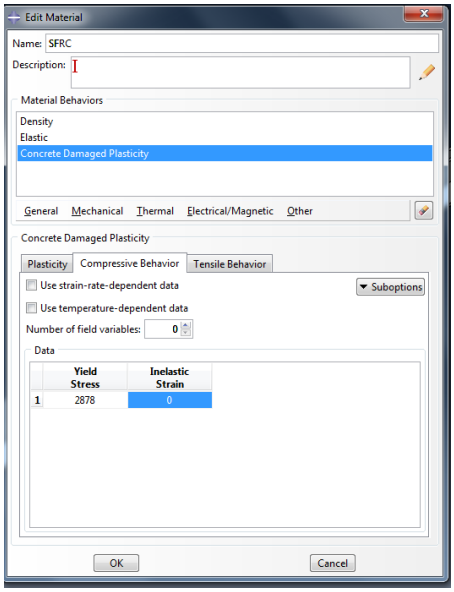

Figure 47. ABAQUS-Material Edit Tool

From the available experiment, for SFRC of 1%, the compressive strength of concrete is 5366 psi, which can be used to determine an Elastic Modulus of 4,175,420 psi. The steel angles are Grade A36 with a yield strength of 36 ksi and an Elastic Modulus of 29000 ksi. Different properties are given for the parametric studies to determine the impact that steel fiber percentage, and or preflex can have on a SFRC encased steel beam. Values from the material properties tests, specifically the compressive strength f_c' and modulus of rupture f_r, are input into ABAQUS for each case. In both parametric studies f_c' and f_r are adjusted according to the 0%, 0.5%, and 1% cases. The Elastic modulus, which also changes according to percent of steel fibers, is also adjusted for each case. The parameters and other physical properties input into ABAQUS can be seen in Table 9.

Table 9.Material Properties of Analyzed Specimens

SFRC Concrete Parametric Study Parameters (PSP)			
% Fibers	0	0.5	1
Compressive strength, f_c (psi)	2878	3832	4277
Modulus Rupture Test, f_r (psi)	609	686	801
Elastic Modulus, E_c (psi)	3093719	3596375	3771911
Angle Steel Joists (Grade A36)			
Yield Stress, f_y (ksi)	36	36	36
Ultimate Stress, f_u (ksi)	73	73	73
Elastic Modulus, E_s (ksi)	29000	29000	29000

4.3.4 Concrete Damage Plasticity

Crack propagation is an important component in studying the flexural behavior of concrete. In order to set bounds for the beam in ABAQUS, tolerance values must be inputted into the Concrete Damage Plasticity (CDP).

Table 10. Concrete Damage Plasticity Parameters [11]

Dilation Angle	Eccentricity	fb0/fc0	K	Viscosity Parameter
31	0.1	1.16	0.667	0

4.3.5 Assembly of Components

After modeling the parts and designating properties, the “Assembly” tool combines each part to form a composite member as shown in Figure 48. The steel angles merge into the SFRC beam in the same manner for each study. Merging the members allows it to become one member that ABAQUS will analyze and still maintain the input properties for each one.

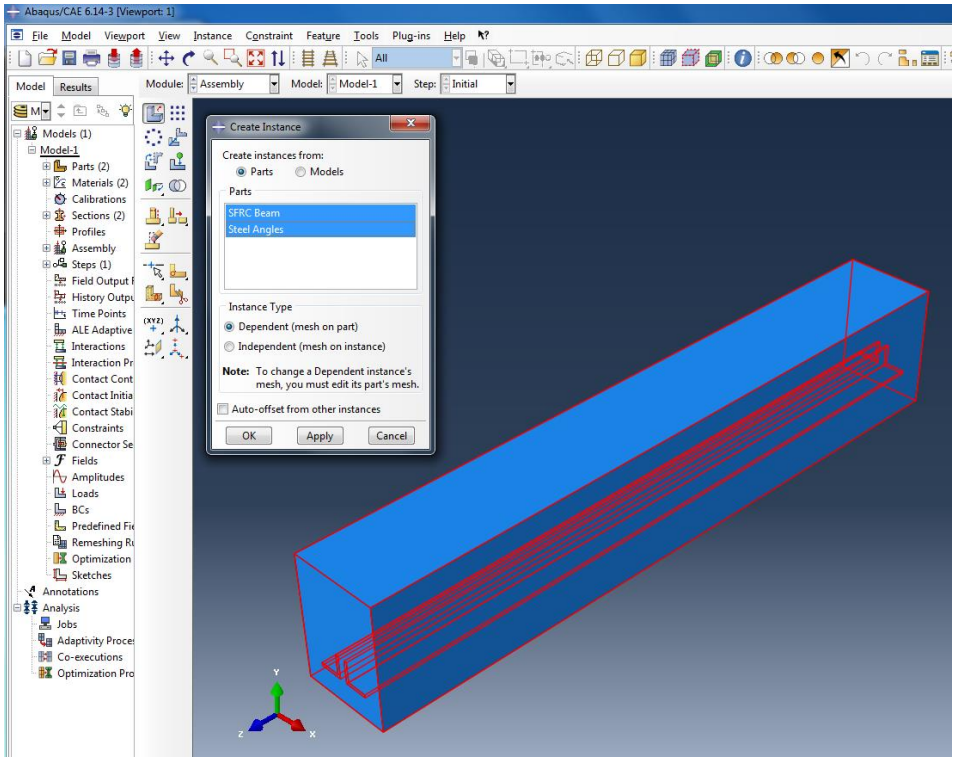

Figure 48.ABAQUS-Assembly of SFRC and Angle Steel

4.3.6 Steps and Time Increments

The step tool defines each analysis step and the output requests for the ABAQUS model. Each step is created and used for the loading process as shown in Figure 49. In this study each step an additional load was added onto the beam to imitate the monotonic loading process used by an actuator in an actual experiment. When creating the step each one has a set increments, which can steadily increase the load up to the point of collapse in 100 smaller steps. This is the automatic setting in ABAQUS as seen in Figure 50.

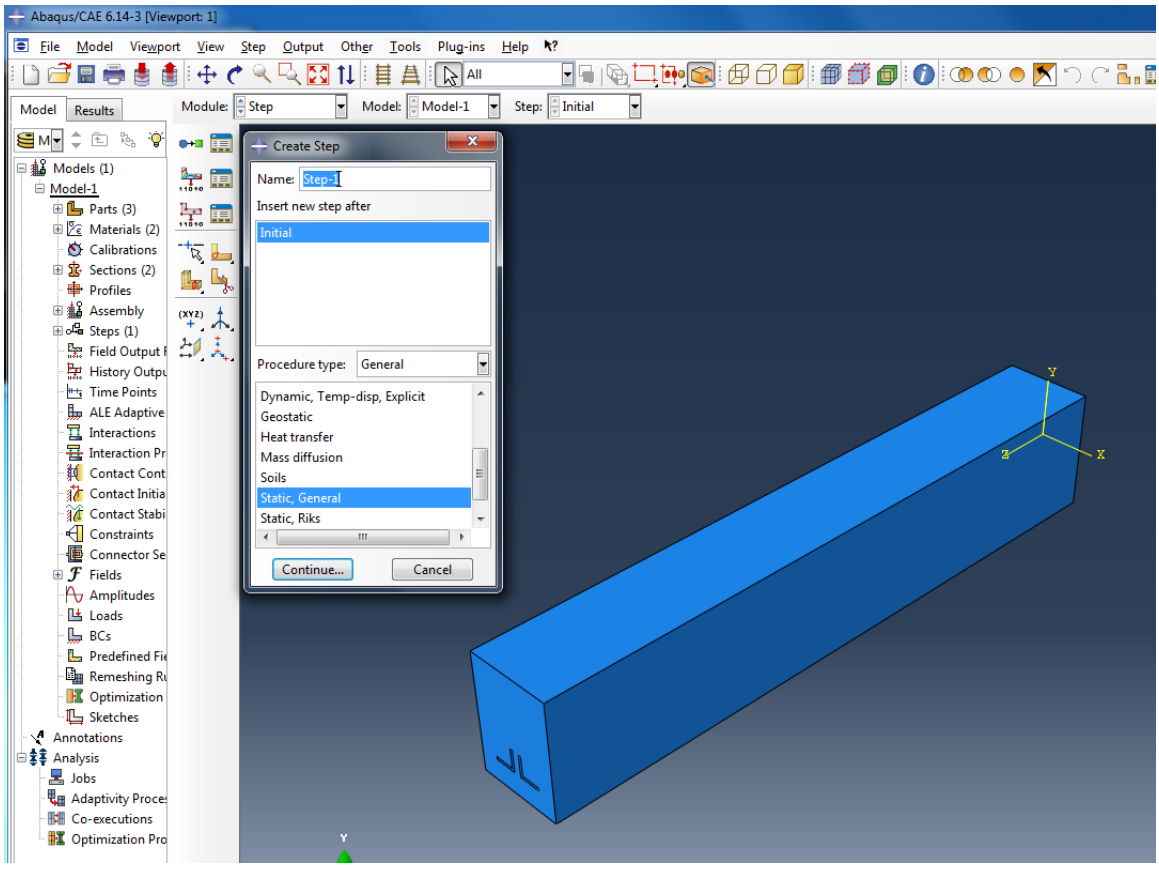

Figure 49. Create Step for each Load

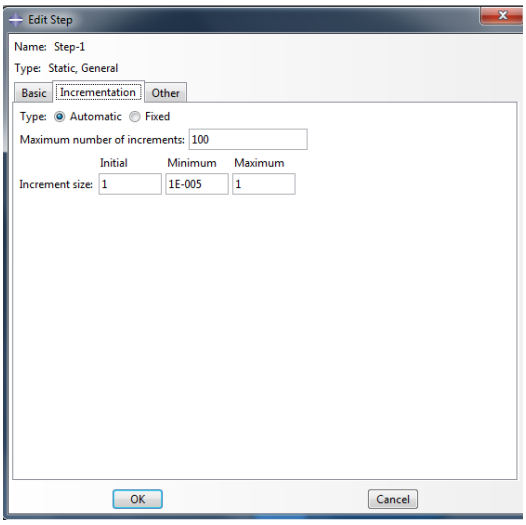

Figure 50. Increments of 100 per Step

4.3.7 Loads and Boundary Conditions

In order to apply a load in ABAQUS, it must be at a designated point. In order to do this for the model, a partition is made at the center as shown in Figure 51. The “Create Partition” tool divides a component into various sections. This tool creates a partition down the middle of the beam, so that a point load could be placed at the center.

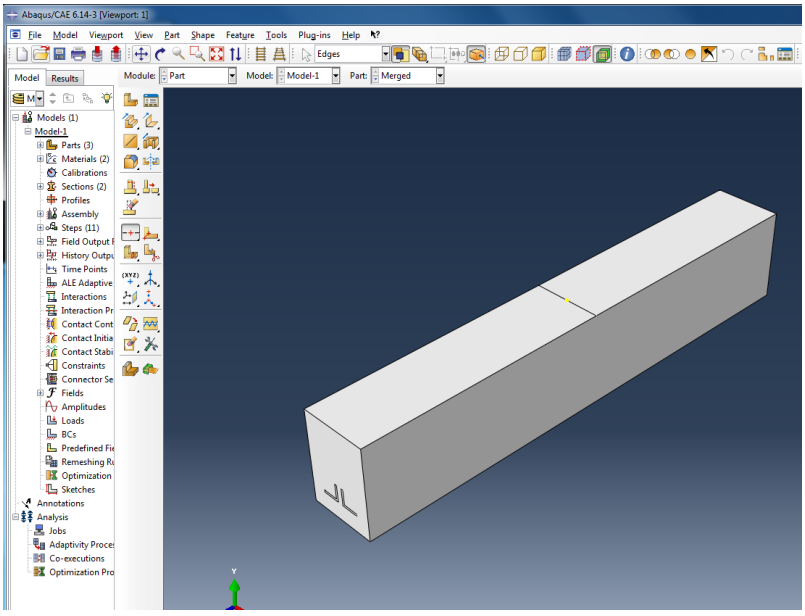

Figure 51. Partition at Center for Loading

A Load is made using the “Create Load” tool as seen in Figure 52. For each step the load act in the downward direction. This is to observe the beam’s behavior in flexure and downward displacement like the available experiment. Loads increase with each step at a rate of 2 kips per step till the beam reaches collapse. The load-step can be adjusted as shown in Figures 53.

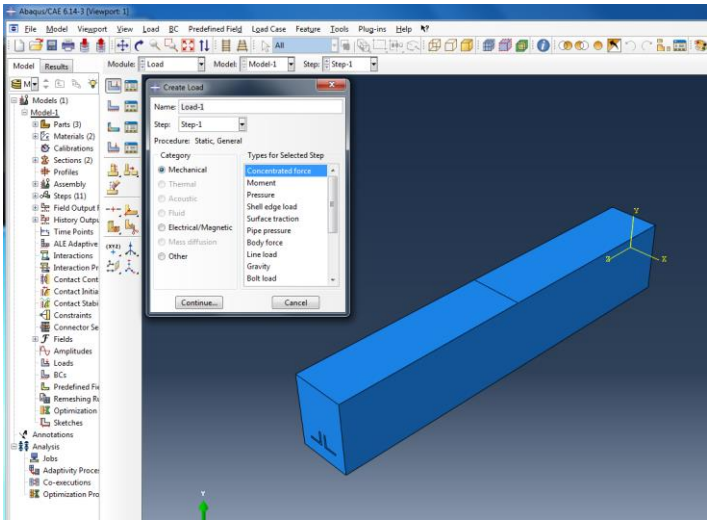

Figure 52. Create a Load for each Step

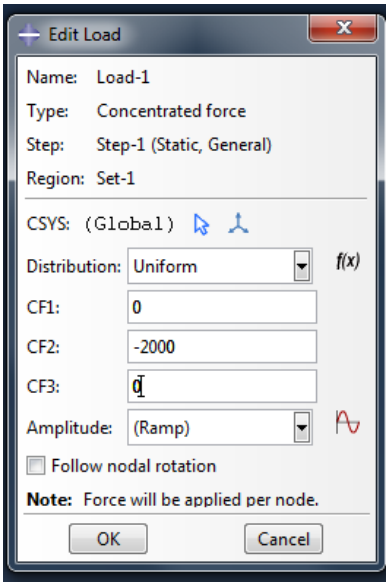

Figure 53.Monotonic Loading of 2 kips

Figures 54-56 are the modeling steps for the Boundary Conditions (B.C.). These restrict certain degrees of freedom (DOF). In this case for a simple supported beam, boundary conditions were placed on each side of the beam in order to imitate a pin-pin connection. This means that the beam can rotate in all axes but

not deflect at the ends. The “Create Boundary Condition” tool allows the user to set the values for the value of displacement at each DOF.

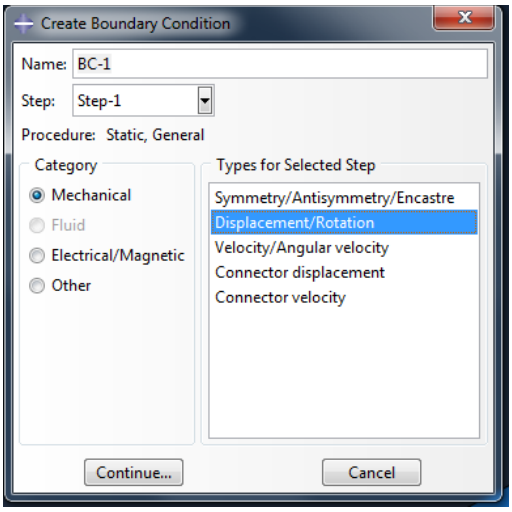

Figure 54. Boundary Condition (B.C.) - Pin-Pin Support

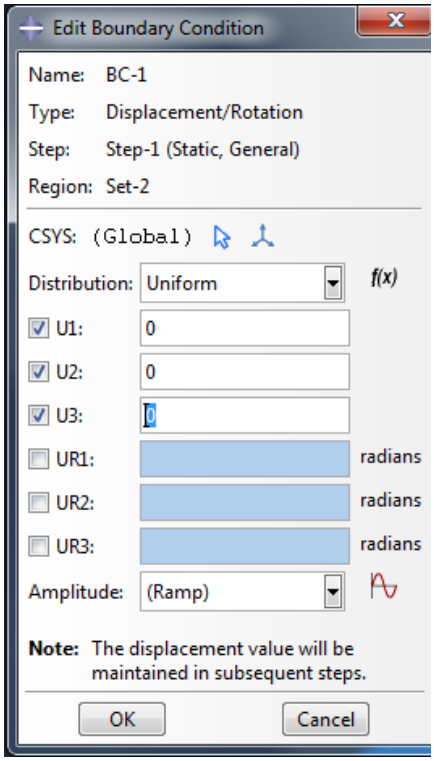

Figure 55. B.C. set to 0 displacement at supports

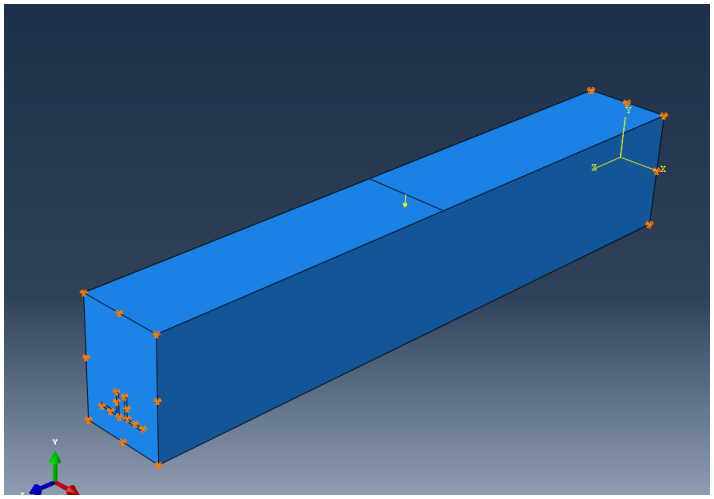

Figure 56. Load and Boundary Conditions for Analysis

4.3.8 3D Visualization

After the job is complete in ABAQUS, the interface allows the user to visualize the results in a 3D display as shown in Figure 57. The change in the model's behavior and physical properties are shown. The regions in the model have different shades of colors to show the distribution of stress and displacement. These results can be put into a graph, which ABAQUS will create for any point on the model.

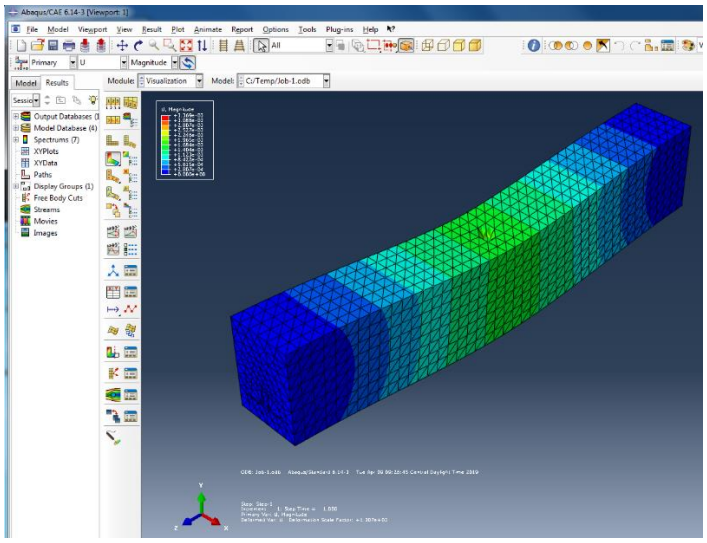

Figure 57. 3D Visualization of Results

Chapter 5

Numerical Analysis

5.1 General

The FEA numerical analysis studies two major objectives. Part one of the study is to confirm the flexural behavior from an available experiment. The second portion of this numerical analysis is the parametric study, which will first investigate straight beams with 0-1% SFRC. The modeled straight beam will be meshed and monotonically loaded in ABAQUS to provide the midspan deflection values. The second part of the parametric study loads the preflex beam in the same manner as the straight beam with the same parameters for 0-1% SFRC to find midspan displacement. For each study the beam is loaded till the collapse point by increments to achieve the most accurate approximation of midspan displacement.

5.2 Mesh Convergence

In order to determine the most approximate amount of displacement experienced in the beam, a mesh convergence study helps to choose the right number of elements. A finer mesh density discretizes the displacement area and the curvature inflection points. A specific geometrical cross section is designed as the mesh depending on the optimal configuration by ABAQUS. Before performing each study, a mesh convergence study is done to confirm what type and dimension of mesh can allow for an accurate representation of the results. The following process helps determine the ideal mesh size in order to achieve an accurate representation of the beam's behavior. Note that Figures 58-60 do not represent the results for this research and only show how the data converges for different mesh sizes.

Figure 58 shows a 0.5"x 0.5" for the Experiment Specimen. This geometry creates an extremely dense model with over 120,000 finite elements. This causes a longer time for the software to process the elements and leads to a poor analysis. The values do not display the available experiment results and do not show convergence. Figure 59 shows a 1"x1" for the Experiment Specimen. The values show the convergence of results, which represent the available experiment results. Figure 60 shows that a 2" by 2" mesh size does not display the results accurately.

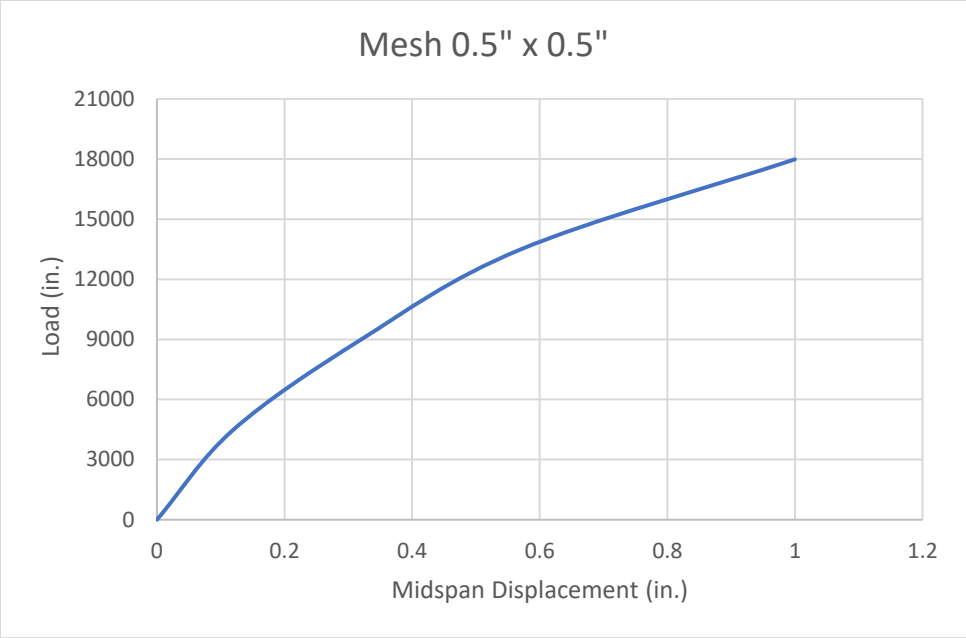

Figure 58. Convergence of .5” by .5” Mesh Size

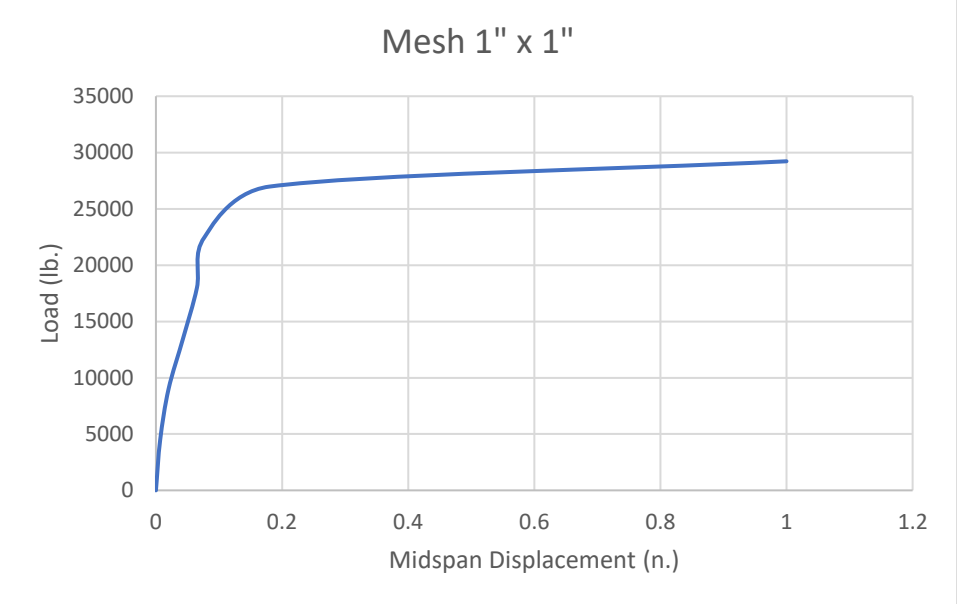

Figure 59. Convergence of 1” by 1” Mesh Size

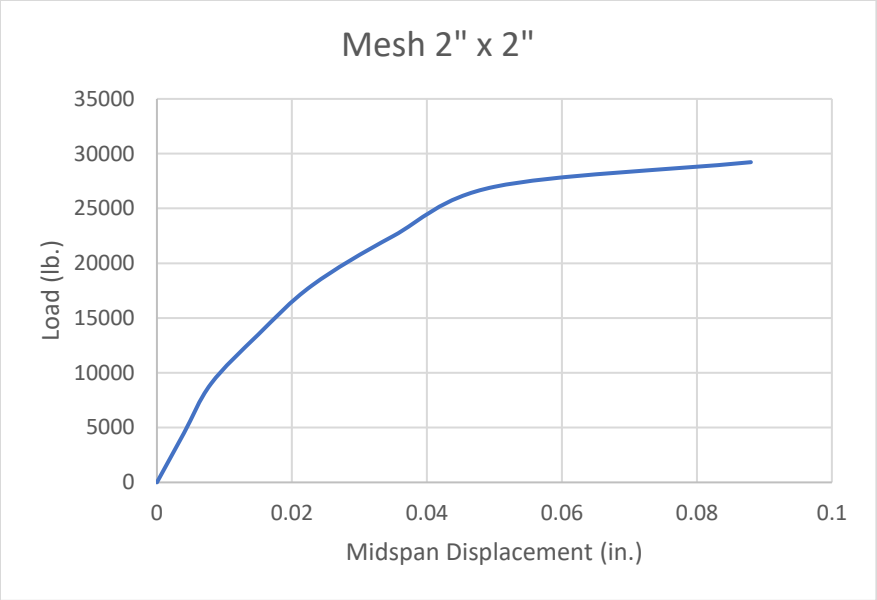

Figure 60. Convergence for 2" by 2" Mesh Size

After analyzing the member with each mesh shown from Figures 58-60, a mesh of 1”x1” was chosen. A mesh of 1”x1” is most optimal in order to determine the collapse load and midspan displacement for each study. Therefore, 20,000 discrete triangular elements will experience the load distribution that contributes to various displacement in different regions of the beam.

The first Finite Element model is “Experiment Specimen”, which represents the specimen from the available experiment under monotonic loading [11]. The second model will be a straight beam for Parametric Study I. The final model will be preflex beam with a camber of .45 inches for Parametric Study II.

5.3 Experiment Specimen Analysis

5.3.1 FEA Results

In the first part of this research, the Khuntia and Goel experiment on a straight SFRC Encased Steel Joist Composite Beam is modeled and analyzed with FEA [11]. The same properties for the SFRC and specimen dimensions from the available experiment are put into the software. The Experiment Specimen analysis is done with the similar load steps as the experiment and compared to the original experiment. Figure 61 shows how ABAQUS displays the flexural behavior of the beam per step. This step shows the beam under a load of 4500 lb.

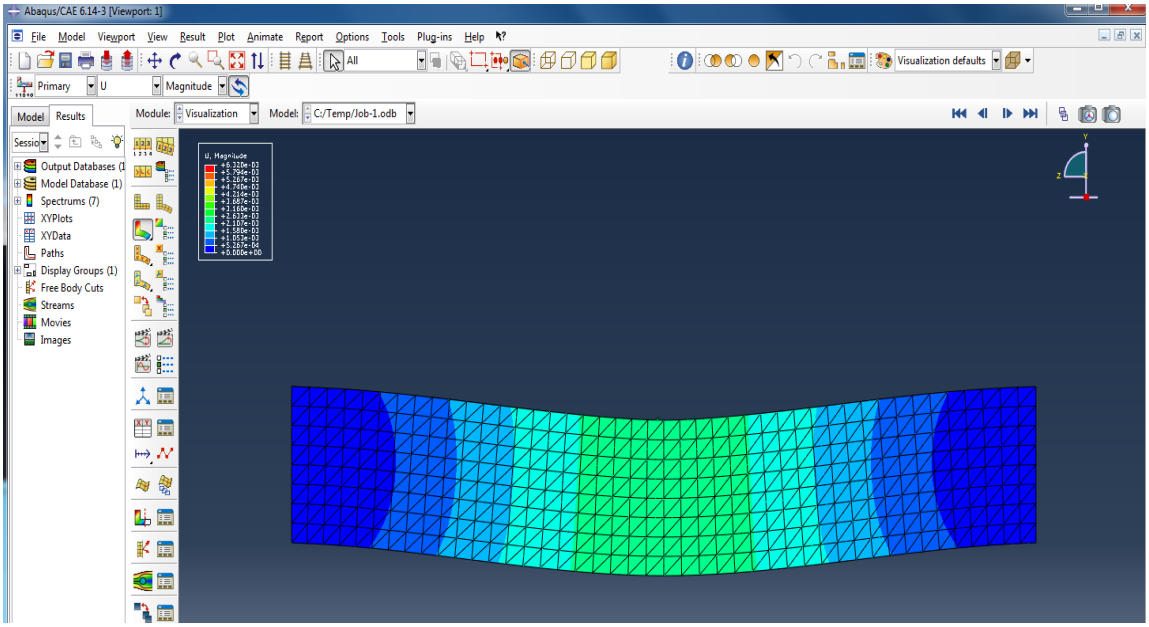

Figure 61.FEA of Experiment Specimen at Initial Load (4,500 lb.)

In FEA the software shows different regions where the displacement is occurring. The software use interpolation to determine a displacement value over a certain number of elements. From Figure 61 the beam can handle the load, but in the midspan region the beam is experiencing the most amount of deflection. This is the regions that is expected to experience the first set of micro cracks. When more load is applied this region should the first part to fail. The change in the Finite Element model from the initial load and the ultimate load will show how the beam goes from this elastic behavior to a plastic deformation.

From the available experiment, the concrete was able to resist a central load up to 27 kips. The crack pattern of the available experiment specimen after final collapse can be seen in Figure 62. The model cracking is shown in Figure 63. In ABAQUS the model experiment specimen shows similar flexural behavior but reaches a cracking point at 22 kips.

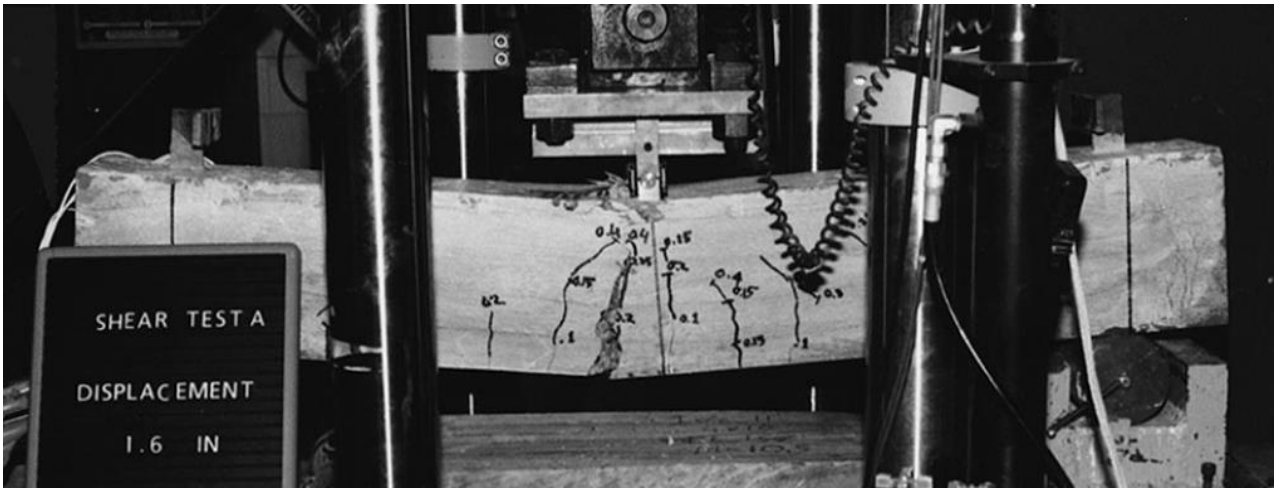

Figure 62.Experiment test of Specimen at Ultimate Load (27 kips)

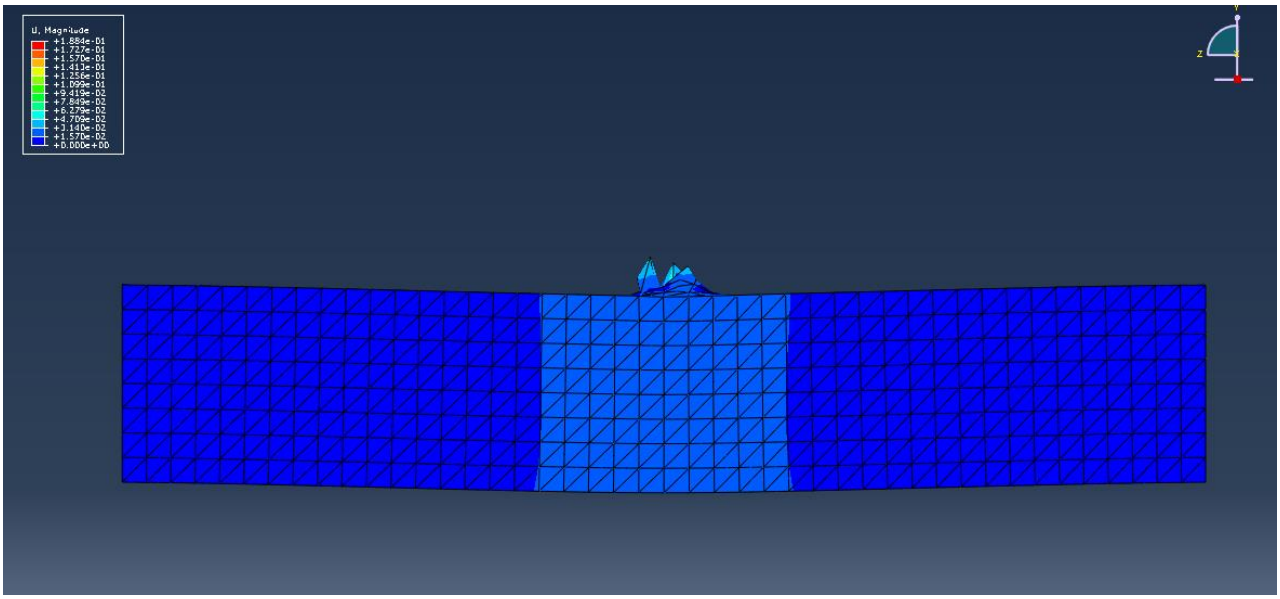

Figure 63. Experiment Specimen Model at Ultimate Load (22kips)

Figure 64 shows how ABAQUS provides a color-coded legend of displacements occurring in specific regions of the beam. This value is the most critical when analyzing the Experiment Specimen and the remaining specimens for each study.

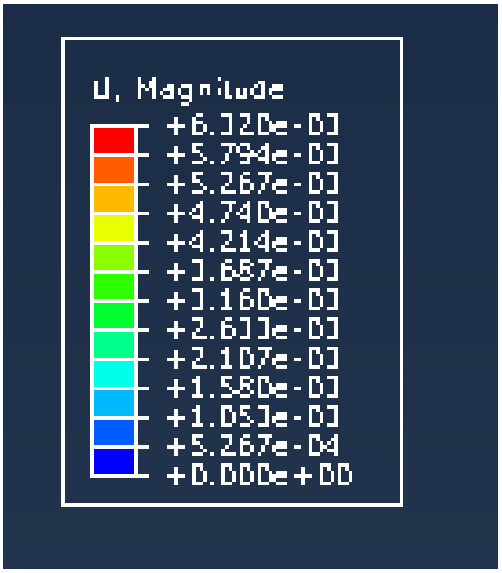

Figure 64. FEA Numerical Analysis Displacement by Region

The displacement values from Figure 64 provide the load-displacement behavior of each beam. The midspan displacement values for the Experiment and Numerical (FEA) after each load step can be seen in Table 11.

Table 11. Midspan Displacement (Experiment vs. Numerical Analysis)

	Midspan Displacement (in.)	
Load (kips)	**Experiment**	**Numerical Analysis**
0	0	0
4.5	0.008	0.0063
9	0.04	0.017
13.5	0.1	0.034
18	0.14	0.065
22.5	0.19	**0.188**
27	0.236	
30	**0.31**	

5.3.2 Load Displacement Curve

Figure 65 shows a comparison of the Experiment and the Numerical (FEA) load-midspan displacement behavior.

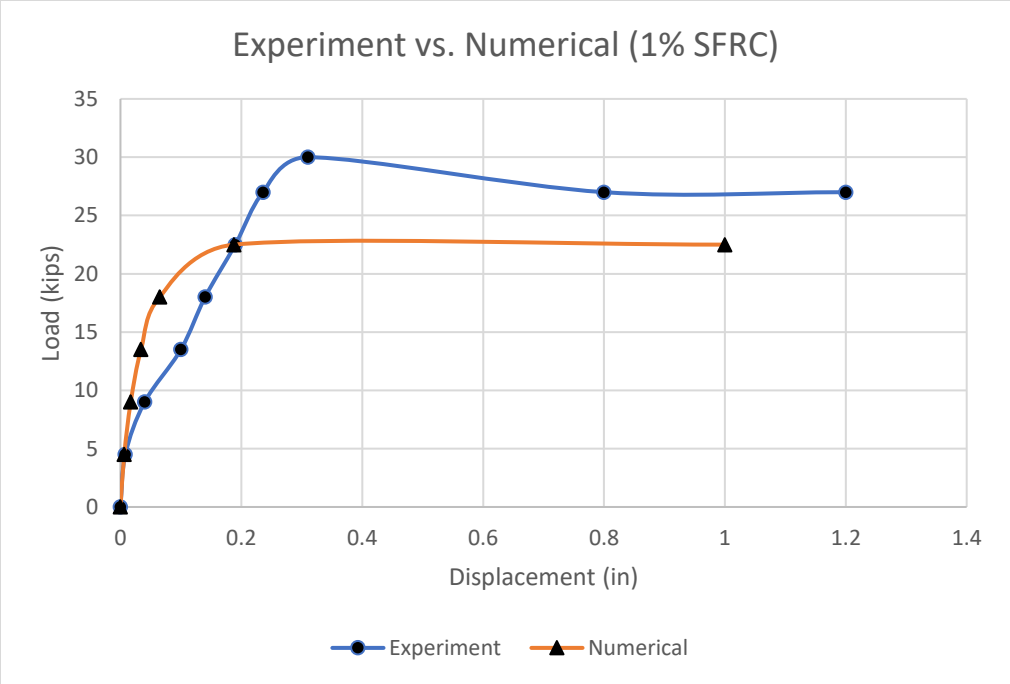

Figure 65. Experiment Specimen Load-Displacement Curve

The load capacity of the specimen from the experiment is around 27 kips, but for the Finite Element model the specimen reaches ultimate strength at 22 kips. There is a 25% difference in the capacities. In the experiment, the specimen reaches a yield displacement of .31 inches [11]. The model experiment specimen reaches its cracking point at .19 inches. FEA does not extend the load cycle past the cracking point because of the Concrete Damage Plasticity limits set. The two curves are close with a 25% difference in displacement values. This is encouraging because although there is a small difference in values, the model still confirms that FEA is close to the results of a real experiment. This part of the study is also critical in order to affirm the parametric parts of this research. Six other Finite Element models are analyzed in the same analysis steps as the Experiment Specimen to give insight on the benefits of Preflex SFRC encased

steel beams. By having knowledge of the realistic displacement that FEA can provide, the software is a trustworthy tool for structural engineering challenges.

5.4 Parametric Study Analyses

5.4.1 Parametric Study I: Straight Beam

The first parametric study investigates how a straight SFRC Encased Steel Joist Composite Beam responds when loaded monotonically by increments of 2 kips. For each load ABAQUS provides the displacement values for different regions of the beam. The load is central on the beam, so the maximum displacement will be at the center. The midspan displacement values from the analysis can be seen in Table 12.

Table 12. Parametric Study I-Midspan Displacement Values

Straight Beam Midspan Displacement (in)			
	Steel Fiber (%)		
Load (kips)	**0**	**0.5**	**1**
0	0	0	0
2	0.0034	0.0068	0.0026
4	0.0086	0.012	0.0062
6	0.015	0.015	0.011
8	0.025	0.018	0.0166
10	0.038	0.027	0.024
12	0.06	0.034	0.033
14	0.094	0.055	0.045
15	**0.46**	0.07	0.05
16		0.081	0.061
18		**0.3**	0.085
20			**0.23**

For the straight beam analyses for 0%, 0.5%, and 1% SFRC, the FEA visualization can be seen from Figures 66-71.

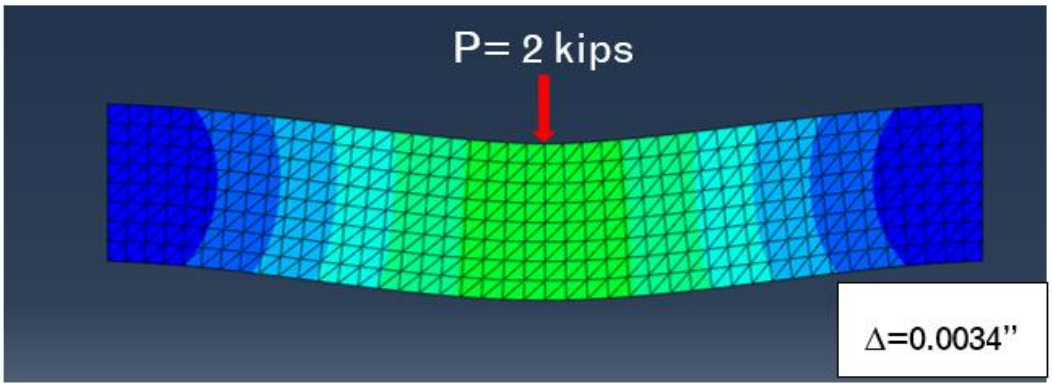

Figure 66. 0% SFRC Straight Beam at Initial Load (2 kips)

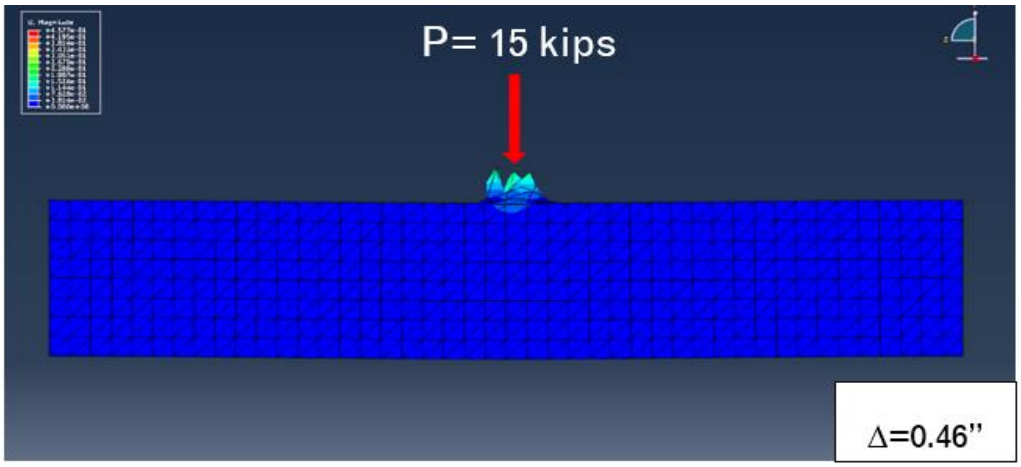

Figure 67. 0% SFRC Straight Beam at Ultimate Load (15 kips)

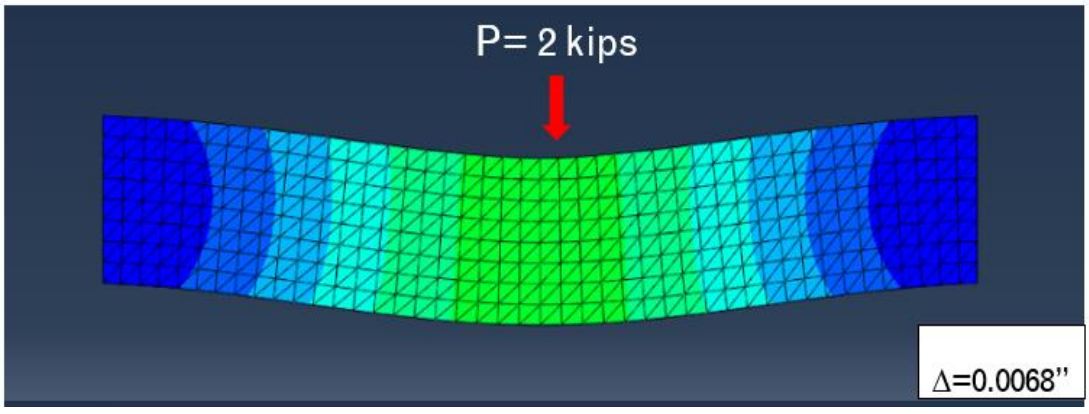

Figure 68. 0.5% SFRC Straight Beam at Initial Load (2 kips)

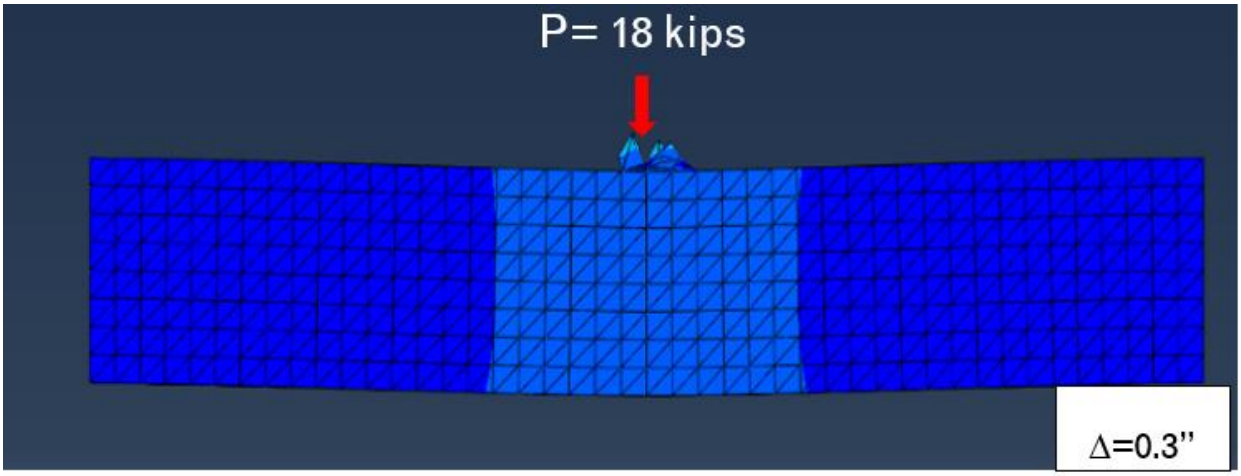

Figure 69. 0.5% SFRC Straight Beam at Ultimate Load (18 kips)

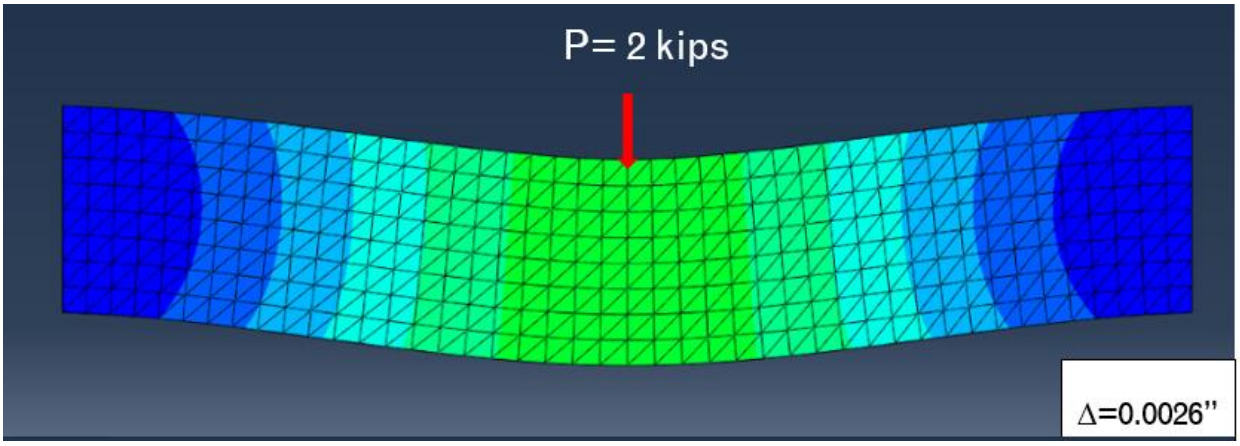

Figure 70. 1% SFRC Straight Beam at Initial Load (2 kips)

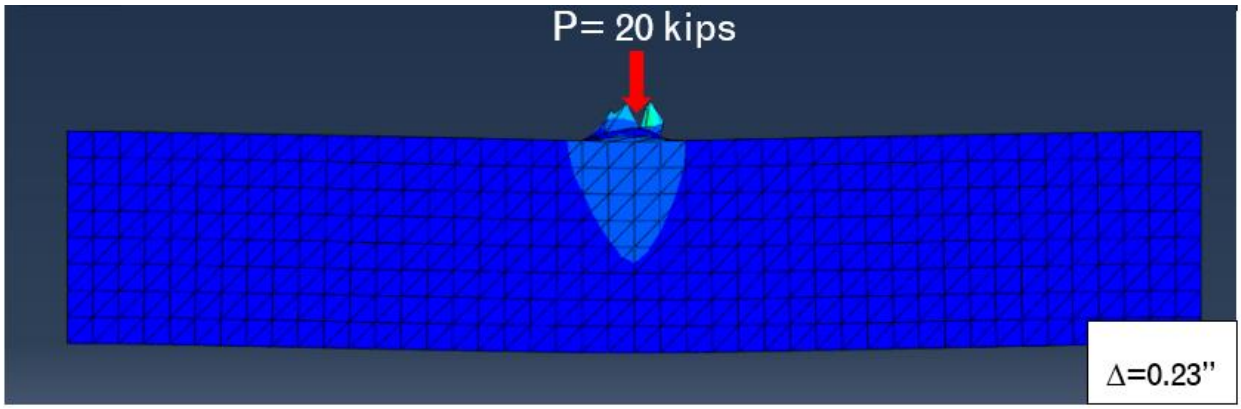

Figure 71. 1% SFRC Straight Beam at Ultimate Load (20 kips)

5.4.2 Parametric Study II: Preflex Beam

For each specimen the f_c' and f_r PSP change to correlate with the straight beam analysis. The specimens are also monotonically loaded by 2 kips per step. Near the point of cracking a smaller load of 1 kip. is used to get a better estimate of the ultimate load capacity. The load-midspan displacement values can be seen in Table 13. FEA provides the cracking point of the beam but does not provide the displacement values after the beam reaches its ultimate strength. The values shown in Table 13 are suitable to study the benefits of preflexing the steel joist in the composite beam. It also shows how adding a higher percentage of SFRC encasement around the steel joist can improve the specimen.

Table 13. Parametric Study II-Midspan Displacement Values

Preflex Beam Midspan Displacement (in)			
	Steel Fiber (%)		
Load (kips)	**0**	**0.5**	**1**
0	0	0	0
2	0.0032	0.0026	0.0025
4	0.0078	0.0062	0.0057
6	0.013	0.01	0.0099
8	0.02	0.016	0.015
10	0.03	0.023	0.02
12	0.044	0.031	0.027
14	0.069	0.042	0.035
16	**0.3**	0.058	0.046
18		0.093	0.061
19		**0.25**	0.072
20			0.087
21			0.13
22			**0.2**

For the preflex beams with .45 inch camber and 0%, 0.5%, and 1% SFRC, the FEA visualization can be seen from Figures 72-77.

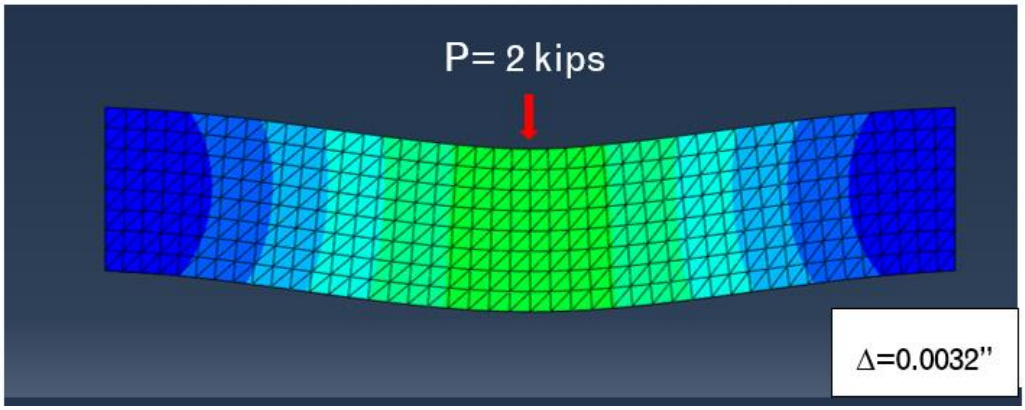

Figure 72. 0% SFRC Preflex Beam at Initial Load (2 kips)

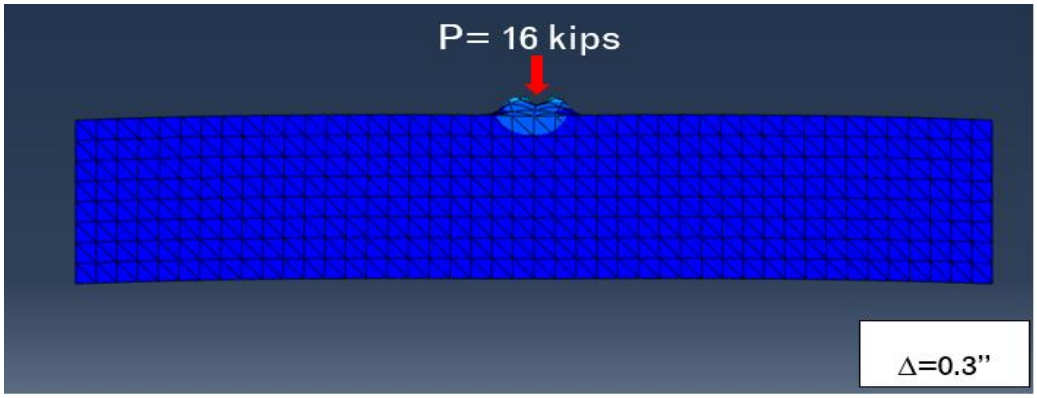

Figure 73. 0% SFRC Preflex Beam at Ultimate Load (16 kips)

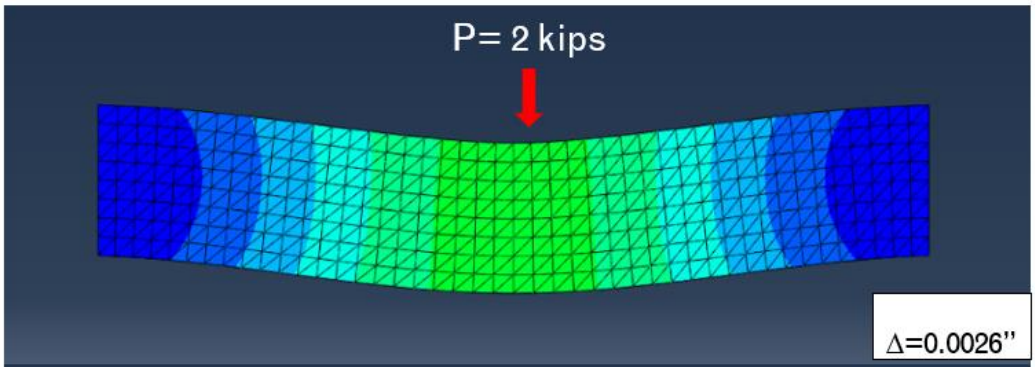

Figure 74. 0.5% SFRC Preflex Beam at Initial Load (2 kips)

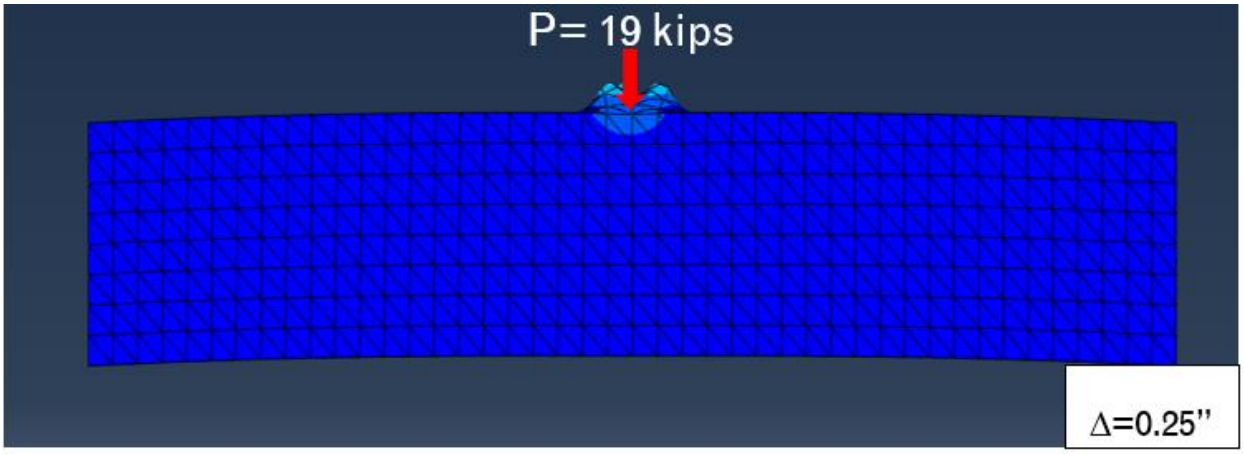

Figure 75. 0.5% SFRC Preflex Beam at Ultimate Load (19 kips)

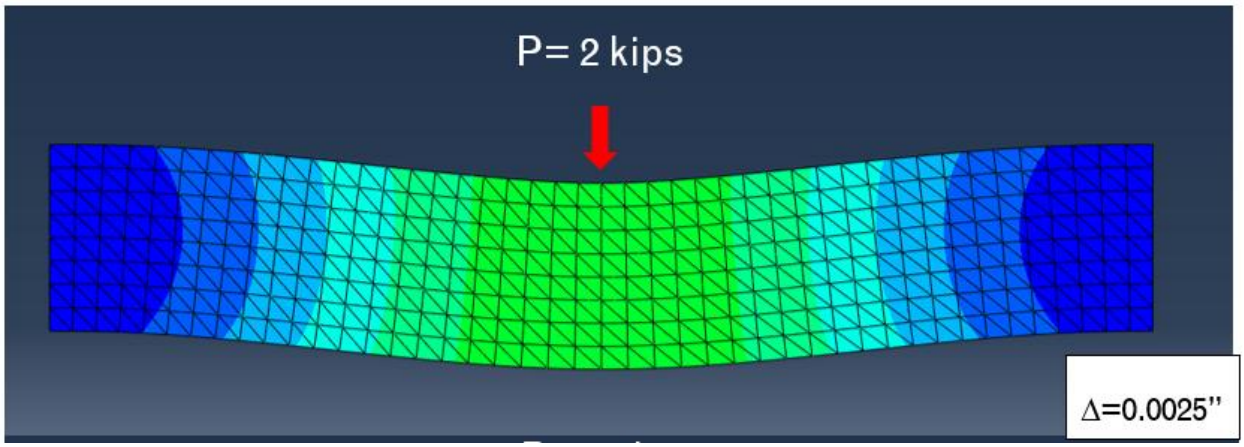

Figure 76. 1% SFRC Preflex Beam at Initial Load (2 kips)

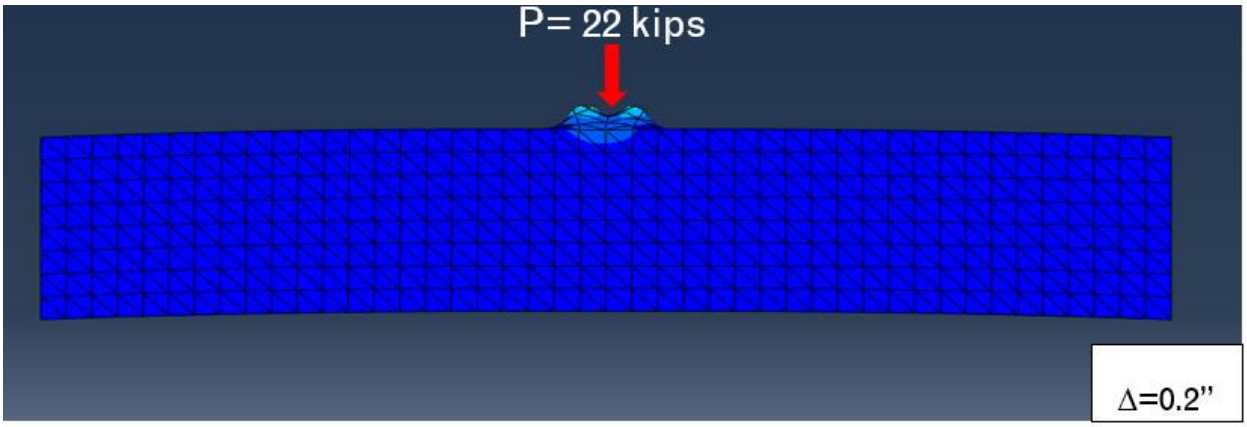

Figure 77. 1% SFRC Preflex Beam at Ultimate Load (22 kips)

5.5 Parametric Study: Load-Displacement Curves

5.5.1 Straight Beam Results

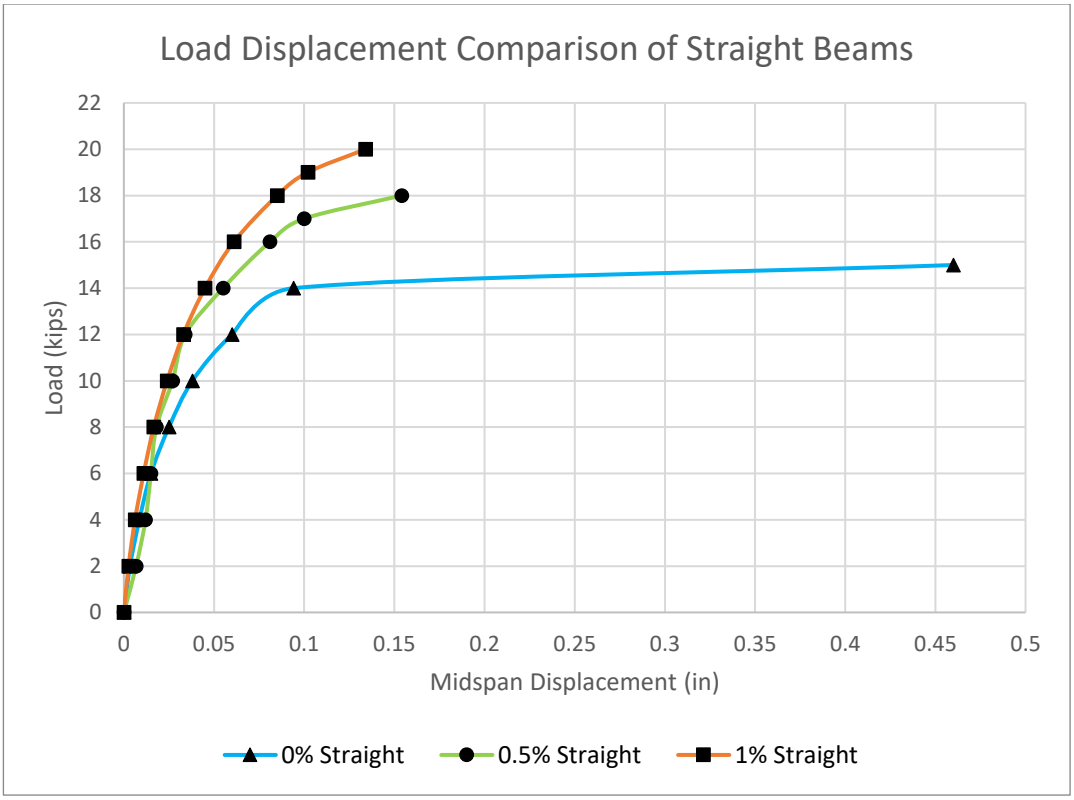

Figure 78. Straight Beam Load Displacement Curve

The load capacities for each straight beam specimen can be seen from Figure 78. The FEA is setup so that for the straight beam specimens the beam is loaded monotonically by 2 kips for 10-12 steps. This load displacement analysis shows that as the percentage of steel fibers increases so does the beam's ability to handle a greater capacity of bending. For 0% SFRC Straight Beam the beam reaches ultimate strength at a load of 15 kips with a maximum displacement of .46 inches. For 0.5% SFRC Straight beam the beam to crack at a greater load capacity of 18 kips and a displacement of .154 inches. For 1% SFRC Straight Beam the beam can handle up to 20 kips with a maximum displacement of .134 inches.

5.5.2 Preflex Beam Results

Three preflex SFRC encased steel beams are monotonically loaded in the same manner as the straight beam study. Each beam has an upwards preflex of .45 inches with the same parameters for compressive

strength and modulus of rupture as the straight beam analysis. Figure 79 shows where each beam reaches its ultimate load and the amount of midspan displacement that results per step.

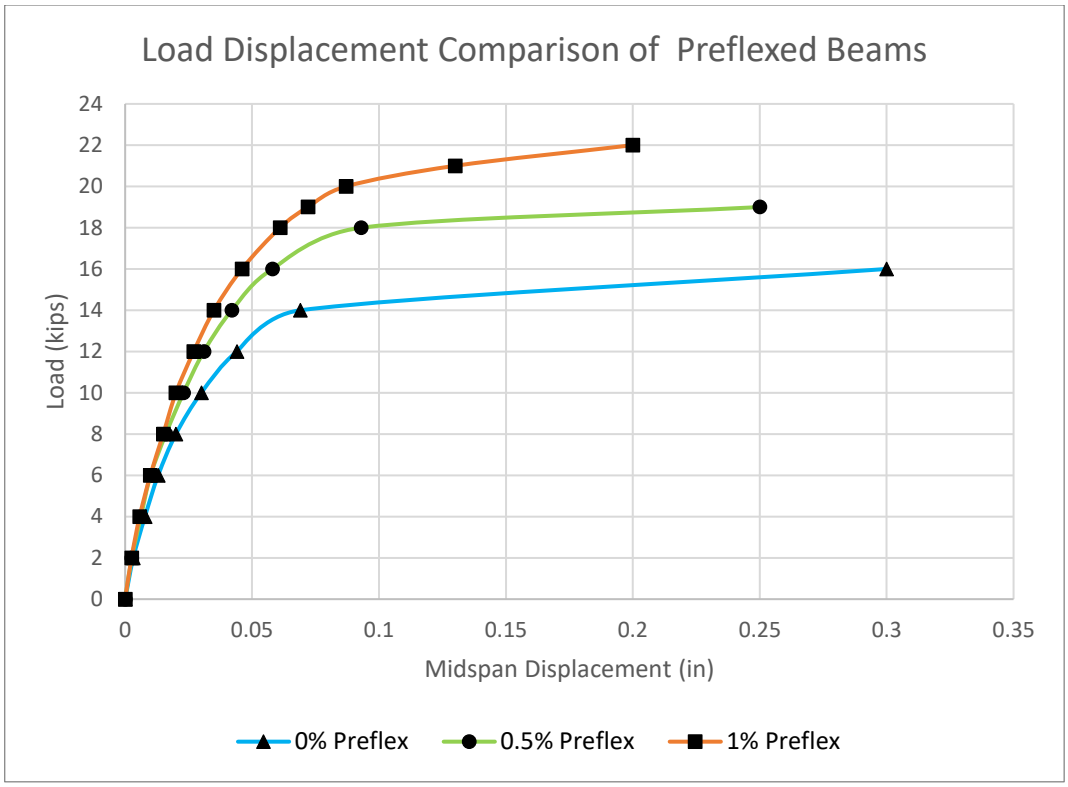

Figure 79. Load-Displacement of Preflex Beams

The 0% SFRC Preflex Beam reaches its ultimate strength at 16 kips with a midspan displacement of .3 inches. The 0.5% SFRC Preflex Beam reaches an ultimate strength of 19 kips with a midspan displacement of .25 inches. The 1% SFRC Preflex Beam cracks at 22 kips with a midspan displacement of .2 inches.

5.5.3 Comparison of Straight vs. Preflex Beams

Figure 80-82 shows the variance in load capacity and midspan displacement between the straight and preflex beams.

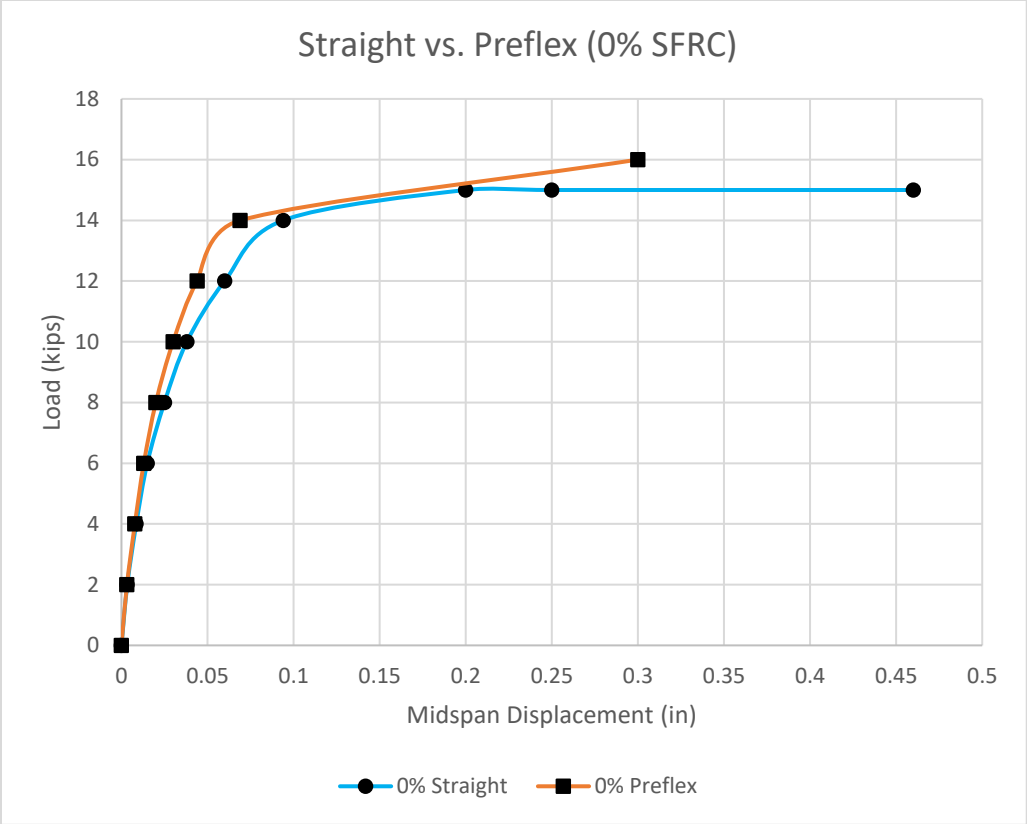

Figure 80. 0% SFRC Load-Displacement Curve

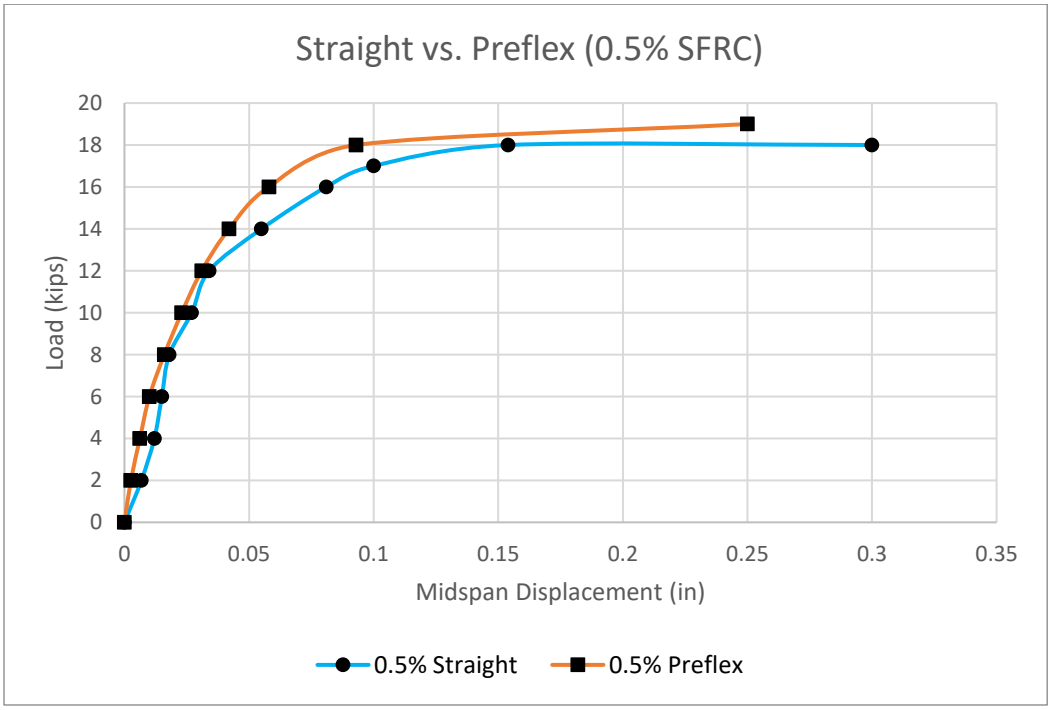

Figure 81. 0.5% SFRC Load-Displacement Curve

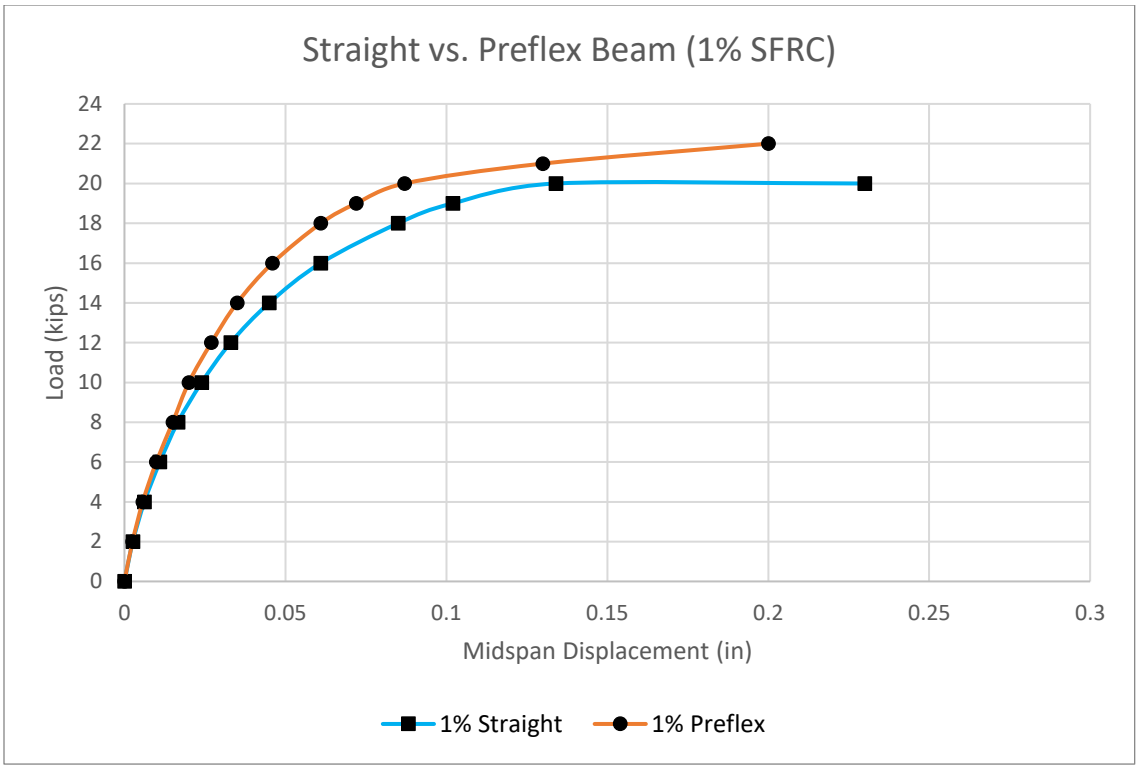

Figure 82. 1% SFRC Load Displacement Curve

From Figure 80, the straight beam experiences .46 inches in total midspan displacement. The preflex beam with a camber of .45 inches is analyzed with the same loading and parameters as the straight beam but only experiences a midspan displacement of .3 inches. In Figures 81 and 82 the midspan displacement continues to decrease as the amount of steel fibers increase. Preflexing also increases the load capacity of the straight beams. In Figure 80 the straight beam reaches an ultimate load of 15 kips, but when preflex the load capacity increases to 16 kips. In Figure 81, the straight beam reaches a load of 18 kips, but when preflex it increases to 19 kips. From Figure 82, the straight beam only reaches 20 kips but when preflex it can handle up to 22 kips.

5.6 Discussion of Results

5.6.1 Experiment Specimen

In the experiment the type of concrete being used is a lot stronger than the concrete that will be used in this numerical analysis. For the Experiment Specimen the numerical analysis is extremely close to the available experiment. The values for the experimental deflection are much larger than the numerical analysis because an actuator (monotonic loading) stops after the maximum displacement. The load is kept for a

longer time to see the point of complete fracture in the experimental analysis, so the collapse point is based on the perspective of the researcher. Due to the realistic oppositions of lab experiments the amount of loading may become inconsistent when compared to a controlled FEA tool such as ABAQUS. From the comparison between FEA and the experiment the percent error is 20% between the displacement and load values. Since the FEA has a small percent of error, it is a suitable tool in approximating the flexural behavior of the experiment SFRC encased steel beam and other beams with different parameters.

5.6.2 Parametric Study Comparison

5.6.2.1 Straight Beams

In the first parametric study, three beams with different SFRC properties are modeled with FEA and monotonically loaded by 2 kips till each reach its ultimate load. Between 0% and 0.5% SFRC the load capacity increases by 20% and the displacement decreases by 60%. Between 0% and 1% SFRC, the load capacity increases by 33% and the midspan displacement reduces by 70%. From Parametric Study I, the FEA shows that by increasing the percent of steel fiber in the SFRC, change in f_c' and f_r has a positive impact in the beam's flexural behavior. The 1% SFRC Straight Beam has the largest increase in the load capacity and the smallest amount of midspan displacement in comparison to the 0% and 0.5% SFRC Straight Beams.

5.6.2.2 Preflex Beams

In the second parametric study, a Finite Element preflex beam with an upwards camber of .45 inches experiences monotonic loading at 2 kips per step. The f_c' and f_r parameters for the preflex beam are consistent with parametric I study for straight beams. Between 0% and 0.5% SFRC the beam's load capacity increases by 20% and the midspan displacement decreases by about 16%. Between 0% and 1% SFRC the load capacity increases by 38% and the midspan displacement decreases by 33%. The FEA shows an increase in steel fibers in a preflex beam will increase the load capacity and decrease the midspan displacement.

5.6.2.3 Straight vs. Preflex Beams

The original intention of making a beam preflex is to enhance its flexural behavior. In this study the preflex beam is meant to increase the load capacity and reduce the midspan displacement. The question is whether

the preflex combined with an increase in steel fiber percentage, will add additional flexural capacity to the specimen. The FEA results improve from the straight to the preflex models. Between 0% SFRC Straight and 0% SFRC Preflex, the preflex beam increases the straight beams load capacity by 7% and reduces its midspan displacement by 35%. Beams 0.5% SFRC Straight and Preflex, the load capacity increases by 6% and midspan displacement decreases by 16%. For beams 1% SFRC Straight and Preflex, the load capacity increases by 10% and the midspan displacement decreases by 13%.

Chapter 6

Conclusion

6.1 Conclusions

- Adding 1% volume fraction of steel fibers into the concrete design mix will increase concrete's compressive strength by 48%, modulus of rupture by 30%, and the tensile strength by 150%.
- The addition of steel fibers into the concrete mix design increases its strength but will reduce the workability.
- The Preflex SFRC Encased Steel Joist Composite beams is a beneficial structural member with enhanced flexural capacity and the ability to reduce midspan displacement significantly.
- For a 0% and 1% SFRC straight beam, the load capacity increases by 33% and the midspan displacement decreases by 70%.
- In comparison of a 1% SFRC straight and preflex beam, the load capacity increases by 10% and the midspan displacement decreases by 13%.
- In comparison of a 0% SFRC straight and preflex beam, the midspan displacement decreases by 35%.
- Overall a 1% SFRC Preflex beam increases a plain concrete straight beam's loading capacity by 47% and reduces its midspan displacement by 60%.
- FEA results are close to the available experiment study on the SFRC encased steel beam with a percent difference of 25%.

6.2 Recommendations for Future Work

- Investigate the behavior of preflex beams with various amounts of upward camber to determine the limits of upward deflection.
- Other studies should explore improving the f_c', f_t , and f_r values by increasing the percentage of steel fibers.
- Perform study with different fiber reinforcement to see the change in mechanical properties of concrete and flexural capacity of preflex beams.
- Analyze a bridge model using FEA to determine the behavior of Preflex SFRC beams under service loads.
- Perform with various preflex steel joist shapes to determine the effect on flexural capacity of the beam.
- Perform study with High Strength SFRC Concrete as an encasement.
- Expand the FEA to graph the post-cracking deformation of the composite beam, so that it shows the behavior after it reaches its ultimate strength.
- Study the cost-analysis of Preflex SFRC beams to determine how the percentage of steel fibers and precambering technology impact design and construction costs.

APPENDIX A:

Sample Calculations & Formulas

a. Compression, Tensile, and Modulus of Rupture Calculations

a. $Compression Strength, f_c' = \frac{P}{\pi r^2}$

P= Load at Failure

r- radius of cylinder

Ex. P=37 kips; r=2 in.

$$\boldsymbol{f_c' = \frac{P}{\pi r^2} = \frac{37000 lbs}{\pi \times 2 in^2} = 2945\ psi}$$

b. $Tensile\ Strength,\ f_t = \frac{2P}{\pi LD}$

P – Compressive Load at Failure

L- Length of Cylinder

D- Diameter of Cylinder

Ex. P=26 kips; L=12 in.; D=6in.

$$\boldsymbol{f_t = \frac{2P}{\pi LD} = \frac{2 \times 26000}{\pi \times 12 \times 6} = 232\ psi}$$

c. $Modulus\ of\ Strength, f_r = \frac{PL}{BD^2}$

P – Load at Failure

L – Beam Span Between Supports

D – Depth of Beam

B – Width of Beam

Ex. P=7 kips; L=20 in.; D= 6in; B=6in.

$$\boldsymbol{fr = \frac{PL}{BD^2} = \frac{(7000 lb.)(20 in.)}{(6 in.)(6 in^2)}}$$

b. Elastic Modulus of Concrete

$$E_c = 57000\sqrt{f_c'}$$

Ex. **0% SFRC:** $\boldsymbol{f_c' = 2878psi}$

$$\boldsymbol{E_c = 57000\sqrt{f_c} = 57000\sqrt{2878} = 3021811\ psi}$$

c. Preflex (Upward Camber) Calculations

a. Upward Deflection

$$\Delta_p = \frac{PL^3}{48EI}$$

b. Bending Moment

$$M = \frac{PL}{4}$$

c. Flexural Stress

$$\sigma = \frac{My}{I}$$

d. By substitution

$$P = \frac{4\sigma I}{Ly}$$

$$\Delta_p = \frac{\sigma L^2}{12Ey}$$

Ex. $\boldsymbol{\sigma = 36000psi; L = 44in; E = 29000\ ksi; y = .45\ in.}$

$$\boldsymbol{P = \frac{4\sigma I}{Ly} = \frac{4(36000psi)(.22in^4)}{(44in)(.45in)} = 1667\ lb.}$$

$$\boldsymbol{\Delta_p = \frac{\sigma L^2}{12Ey} = \frac{(36000psi)(44^2)}{12(29000000)(.45\ in)} = .45\ in.}$$

References

[1] AASHTO “AASHTO Load and Resistance Factor Design (LRFD) Bridge Design Specifications,” eight edition, American Association of the State Highway and Transportation Officials, Washington DC, 2017.

[2] Abaqus 6.11 Theory Manual (2011).

[3] ACI Committee 318. Building Code Requirements for Structural Concrete : (ACI 318-14) ; and Commentary (ACI 318R-14). Farmington Hills, MI :American Concrete Institute, 2014.

[4] Ahmadullah, N., Shimozato, T., & Masayuki T. (2017). “A Study on Application of Elastic Theory for Computing Flexural Stresses in Preflex Beam” *International Journal of Structural and Construction Engineering* Vol. 11 (10), pp 1365.

[5] ASTM C39 Test Method for Compressive Strength of Cylindrical Concrete Specimens

[6] ASTM C78 Test Method for Flexural Strength of Concrete

[7] ASTM C192 Standard Practice for Making and Curing Concrete Test Specimens

[8] ASTM C496 Test Method for Splitting Tensile Strength of Cylindrical Concrete Specimens.

[9] Azzawi, Dr. R. K, & Jafar, Y.S. (2009). “Nonlinear Analyses of Composite Preflex Steel Beams Encased in Concrete” *Journal of Engineering* Vol. 15, pp. 3868-3889.

[10] Clough, R. W. (2004). “Early History of the finite element method from the view point of a pioneer” *International Journal for Numerical Methods in Engineering.* Vol. 60, pp. 283-287.

[11] Ghori, M. (2017). “Non-linear Analysis of Steel Fiber Reinforced Concrete Hollow Columns Under Uniaxial Bending” Master of Science Thesis. The University of Texas Arlington.

[12] Grace, N., Ushijima, K., Matsagar, V., & Wu, C. (2013). “Performance of AASHTO-Type Bridge Model Prestressed with Carbon Fiber-Reinforced Polymer Reinforcement” *ACI Structural Journal.* Vol. 110 No. 3. pp 1-10.

[13] Josef Hegger, and Clause Goralski, "Structural Behavior of Partially Concrete Encased Composite Sections with High Strength Concrete", Composite construction in steel and Concrete, 2006. pp. 311-346.

[14] Khuntia, M & Goel, S.C. (1999). “Experimental Study of FRC-Encased Steel Joist Composite Beams” *Journal of Structural Engineering.,* ASCE, Vol. 125 (5). pp. 495-500.

[15] Kvocak, V., Tomko, M., & Kozlejova, V. (2013). “Modeling of Encased Steel Beams in ABAQUS Program” *International Conference on Intelligent Engineering System*. pp. 255-259.

[16] Lok, Tat-Sneg & Pei, Jin-Song. (1998). “Flexural Behavior of Steel Fiber Reinforced Concrete” *Journal of Materials in Civil Engineering.,* ASCE Vol. 10 No. 2. pp 86.

[17] Mahadik, S. A., Kamane, S. K., Lande A. C. (2014). “Effect of Steel Fibers on Compressive and Flexural Strength of Concrete” *International Journal of Advanced Structures and Geotechnical Engineering* Vol.3 No. 4. pp 388-392.

[18] Mannini, C., & Morano, S.G. (2006). “Preflex Beams: Structural Optimation and analysis of economic advantges”. University of Florence, Italy.

[19] Mohite, P. M. “History of FEM-Origin of FEM” IIT Kanpur.

[20] Song, P.S. & Hwang, S. (2004). “Mechanical Properties of High Strength Steel Fiber-Reinforced Concrete” *Construction and Building Materials.* Vol. 18. pp. 669-673.

[21] Weck, O. (2005). “CAE-Finite Element Method” Massachusetts Institute of Technology.

[22] Zoli, T. P. & Steinhouse, J. “Some Considerations in the Design of Long Span Bridges Against Progressive Collapse”.

[23] Zsuza P. (2014). “PREFLEX girders: Prefabricated composite bridges” *The Journal of the Hungarian Steel Association.* pp 1-10.